Improvement of Physiochemical Properties of the Tetrahydroazepinoindole Series of Farnesoid X Receptor (FXR) Agonists: Beneficial Modulation of Lipids in Primates[†]

Joseph T. Lundquist, IV,*,[§] Douglas C. Harnish,*,[‡] Callain Y. Kim,[§] John F. Mehlmann,[§] Rayomand J. Unwalla,[§] Kristin M. Phipps,[§] Matthew L. Crawley,[§] Thomas Commons,[§] Daniel M. Green,[§] Weixin Xu,[#] Wah-Tung Hum,[#] Julius E. Eta,[∥] Irene Feingold,[∥] Vikram Patel,[∥] Mark J. Evans,[‡] KehDih Lai,[‡] Lisa Borges-Marcucci,[‡] Paige E. Mahaney,[§] and Jay E. Wrobel[§]

[§]*Department of Chemical Sciences,* [‡]*Cardiovascular and Metabolic Diseases, and* [∥]*Drug Safety and Metabolism, Wyeth Research, 500 Arcola Road, Collegeville, Pennsylvania 19426, and* [#]*Department of Chemical Sciences, Wyeth Research, 200 Cambridge Park Drive, Cambridge, Massachusetts 02140*

In an effort to develop orally active farnesoid X receptor (FXR) agonists, a series of tetrahydroazepinoindoles with appended solubilizing amine functionalities were synthesized. The crystal structure of the previously disclosed FXR agonist, **1** (FXR-450), aided in the design of compounds with tethered solubilizing functionalities designed to reach the solvent cavity around the hFXR receptor. These compounds were soluble in 0.5% methylcellulose/2% Tween-80 in water (MC/T) for oral administration. In vitro and in vivo optimization led to the identification of **14dd** and **14cc**, which in a dose-dependent fashion regulated low density lipoprotein cholesterol (LDLc) in low density lipoprotein receptor knockout (LDLR$^{-/-}$) mice. Compound **14cc** was dosed in female rhesus monkeys for 4 weeks at 60 mg/kg daily in MC/T vehicle. After 7 days, triglyceride (TG) levels and very low density lipoprotein cholesterol (VLDLc) levels were significantly decreased and LDLc was decreased 63%. These data are the first to demonstrate the dramatic lowering of serum LDLc levels by a FXR agonist in primates and supports the potential utility of **14cc** in treating dyslipidemia in humans beyond just TG lowering.

Introduction

The farnesoid X receptor (FXR)[a] is a member of the metabolic nuclear receptor superfamily of regulatory proteins and is highly expressed in the liver, kidney, and intestine.[1] It is activated by bile acids (e.g., chenodeoxycholic acid, CDCA, and cholic acid, CA), the final products of cholesterol catabolism.[2] Functionally, activated FXR binds with high affinity to an inverted repeat-1 (IR-1) response element on DNA as a heterodimer with the retinoid X receptor (RXR).[3] This binding event regulates the expression of various transport proteins and biosynthetic enzymes that maintain cholesterol and bile acid homeostasis.[4] Additionally, FXR regulates the expression of a number of genes involved in triglyceride synthesis[5] and lipogenesis.[6] Although FXR was only identified as a receptor for bile acids in 1999, a link between bile acids and triglycerides was made more than 30 years ago when patients on CDCA treatment for gallstone dissolution were concomitantly observed to have reduced levels of serum triglycerides.[7] Separately, patients with familial hypertriglyceridemia (FHTG) were found to have a defect in bile acid absorption in the ileum,[8] and patients on cholesterol-lowering bile acid sequestrants exhibited a marked increase both in serum triglycerides and in hepatic very low density lipoprotein (VLDL) production.[9] While this evidence strongly supports a role of FXR in the triglyceride lowering effects of CDCA and substantiates FXR agonists as attractive therapies for hypertriglyceridemia, researchers do not fully understand the effect of FXR activation on cholesterol homeostasis. On one hand, since activation of the receptor by its endogenous ligands results in a decrease in cholesterol metabolism through a reduction in expression of cholesterol 7α-hydroxylase (cyp7a1),[10] treatment with synthetic FXR agonists could potentially increase overall cholesterol concentrations. On the other, since bile acid-mediated activation of FXR has been shown to increase the abundance of ABCG5 and ABCG8, hepatic transporters that are required for biliary cholesterol secretion,[11] treatment with FXR agonists could potentially decrease total cholesterol levels. Previously, we demonstrated dramatic effects on lipoprotein profiles with the

---

[†]The atomic coordinates of the FXR-ligand-binding domain complexed with **14cc** have been deposited in the RCSB Protein Data Bank, www.rcsb.org (PDB code 3L1B).

*To whom correspondence should be addressed. (J.T.L.) Tel: 484-865-2730. Fax: 484-865-9399. E-mail: lundquj@wyeth.com. (D.C.H.) Tel: 484-865-7459. Fax: 484-865-7459. E-mail: harnisd@wyeth.com.

[a] Abbreviations: FXR, farnesoid X receptor; hFXR, human FXR; mFXR, mouse FXR; RXR, retinoic acid X receptor; RCT, reverse cholesterol transport; FAS, fatty acid synthase; FHTG, familial hypertriglyceridemia; CDCA, chenodeoxycholic acid; CA, cholic acid; 6-ECDCA, 6-ethyl-chenodeoxycholic acid; LDL, low density lipoprotein; LDLc, low density lipoprotein cholesterol; VLDL, very low density lipoprotein; VLDLc, very low density lipoprotein cholesterol; HDL, high density lipoprotein; HDLc, high density lipoprotein cholesterol; TG, triglyceride; LDLR$^{-/-}$, low density lipoprotein receptor knockout; cyp7a1, cholesterol 7α-hydroxylase; cyp8b1, sterol 12α-hydroxylase; SHP, short heterodimer partner; LBD, ligand-binding domain; HEK, human embryonic kidney; PK, pharmacokinetic; PD, pharmacodynamic; FPLC, fast performance liquid chromatography; MC/T, 0.5% methylcellulose/2% Tween-80 in water; EtOAc, ethyl acetate; EDC, 1-ethyl-3-(3-dimethylaminopropyl) carbodiimide hydrochloride; DEAD, diethylazodicarboxylate; DIAD, diisopropylazodicarboxylate.
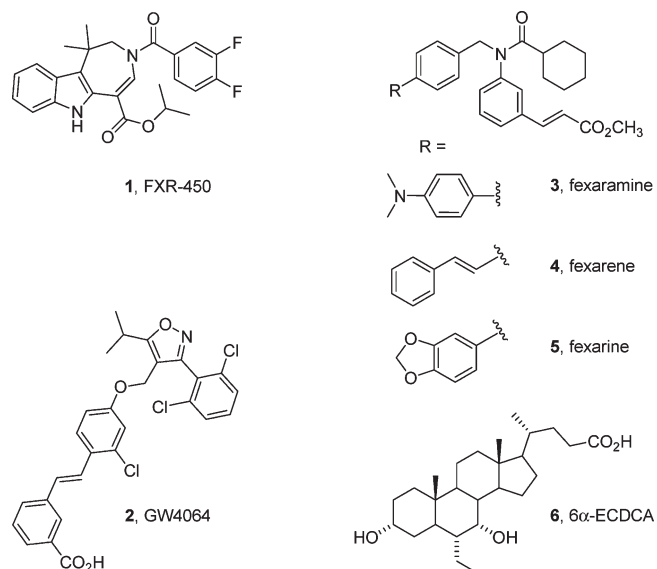
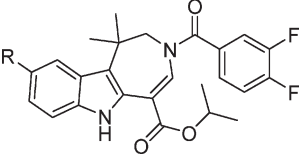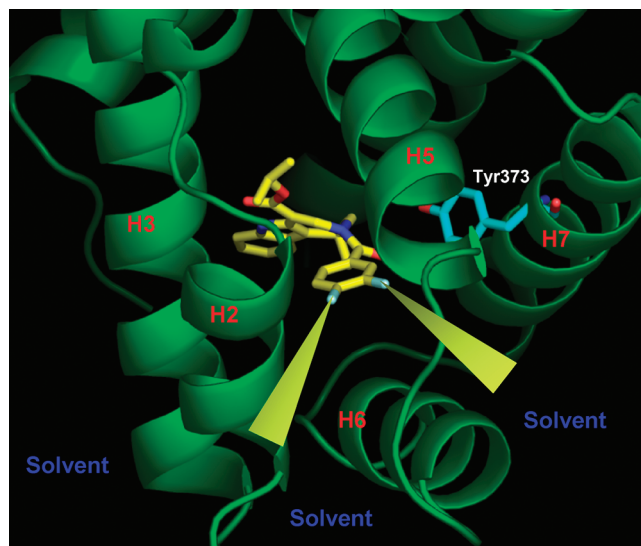**Figure 1.** Structures of synthetic FXR agonists.

Figure 2. X-ray structure of **1** occupying hFXR-LBD. Helices discussed in the text are numbered H1−H12. Yellow vectors indicate general direction (meta (3-position) or para (4-position) attachment on the benzoyl functionality) for tethering solubilizing functionalities to solvent cavity past helix-2.

FXR agonist, **1** (FXR-450),[12] in dyslipidemia models in mice, rats, and hamsters, in which the regulation on LDLc and high density lipoprotein cholesterol (HDLc) levels may be both model and species specific. However, in all models, regulation of genes involved in the reverse cholesterol transport (RCT) pathway and cholesterol synthetic pathways was observed. Taken together, the data suggest that synthetic, nonsteroidal FXR modulators may be beneficial for the treatment of a variety of metabolic disorders including hypertriglyceridemia, dyslipidemia, and gallstones without the toxicity that is associated with bile acids.

Several other research groups have focused on the identification of synthetic FXR agonists. Maloney et al. discovered the first high affinity, nonsteroidal FXR agonist **2** (GW4064),[13] with an EC_{50} value of 37 nM. Although this compound suffered from poor oral bioavailability, it served as a chemical tool to demonstrate triglyceride (TG) lowering in rats. Natural product-like libraries provided hits for Nicolaou et al. that were optimized into a number of potent FXR agonists including fexaramine, fexarene, and fexarine (**3**, **4**, and **5**, respectively, Figure 1),[14] and Pelliccari et al. optimized CDCA, a weak activator of FXR with an EC_{50} value of 8.7 μM, into 6-ethyl-chenodeoxycholic acid **6** (6-ECDCA), a potent FXR agonist exhibiting an EC_{50} value of 99 nM.[15] Compound **6** is currently being evaluated in the clinic for the treatment of cholestatic liver disease but has reduced chronic utility due to a small therapeutic window. While progress has been made toward the identification of potent FXR agonists, significant limitations associated with these compounds increase the need for newer ligands with improved ADME properties and good safety profiles to allow clinical evaluation of this class of potential drugs for chronic indications.

Recently, **1** (Figure 1), containing a novel azepino[4,5-*b*] core, was disclosed as a potent and selective FXR agonist that advanced to clinical trials.[16] The highly lipophilic character of **1** (*c*Log *P* = 5.30), which is necessary to interact favorably with the hydrophobic ligand-binding domain (LBD) of human FXR, required the use of an unusual nonaqueous vehicle (corn oil) for oral dosing. To potentially decrease lipophilic character while maintaining favorable agonist interaction, we recently reported on a series of truncated pyrrole[2,3-*d*]azepino with lower *c*Log *P*s, ranging from 3.18 to 4.91.[17]

While these truncated analogues were very potent and efficacious hFXR agonists, they did not show an improvement in aqueous solubility in pH 7.4 buffer (solubility of all analogues tested was below the limit of detection). The X-ray crystal structure of **1** suggested that to attain solubility in a pharmaceutically acceptable vehicle the introduction of polar functionalities would be challenging. Given the highly lipophilic LBD, it was envisioned that solubilizing functionalities might be tolerated if they were tethered away from the lipophilic azepino[4,5-*b*] core occupying LBD, toward the solvent cavity past the flexible helix-2. The proposed points for attachment are indicated with yellow vectors showing the direction for solubilizing functionalities to reach solvent from the meta (3-position) or para (4-position) on the benzoyl functionality (Figure 2).

During the design process, we also focused on trying to improve microsome stability of **1** by incorporating a fluorine atom into the 9-position of the azepino[4,5-*b*] core. Using previously described methodology,[16] analogue **7** was prepared (Table 1). Liver microsomal stability assays[18] revealed that the fluorination in **7** provided improved stability over the *des*-fluoro azepino[4,5-*b*] core in **1**, while maintaining similar hFXR and mFXR potency and efficacy. We planned to use the strategy of introducing fluoro and other electron-deficient blocking groups in either the 8- and 9-positions of compounds with pendant solubilizing functionalities. This would hopefully confer added stability combined with improved solubility.

Chemistry

For incorporation of appended solubilizing groups, we first explored a series of alkylated basic amines with a range of basicity to allow the possibility of formulation improvement via salt preparation. A parallel approach for the synthesis was designed in which diversity elements could be incorporated in the last one or two steps of the synthesis. In Scheme 1, the benzoyl functionality containing the point of tether attachment was incorporated through acylation of the nitrogen in core molecules **8** or **9**. This provided intermediates with a C-linked tether (**10a−10h**) and benzyl-protected phenols

Table 1. Effect on FXR Functional Activity and Microsome Stability for 9-Fluoro Substitution on Azepino[4,5-*b*] Analogues

compound	R	hFXR EC_{50}^a (nM)	efficacy in hFXR[b] (%)	mFXR EC_{50}^c (nM)	efficacy in mFXR[b] (%)	stability (human)[d] $t_{(1/2)}$ min	stability (mouse)[d] $t_{(1/2)}$ min
1	H	15 ± 6	141 ± 22	152 ± 86	174 ± 81	20	13.5
7	F	45 ± 8	150 ± 27	112 ± 37	90	> 30	> 30

[a] Induction of human FXR measured in HEK293 stable clones expressing Gal4/human FXR-LBD. [b] Efficacy = [maximal fold induction of test compound/maximal fold induction of compound **2** × 100]. [c] Induction of mouse FXR measured in HEK293 stable clones expressing Gal4/mouse FXR-LBD. [d] Liver microsomal.

Scheme 1. Parallel Synthesis of Azepino[4,5-*b*]indoles with Carbon-Linked Pendant Amines **11a−h** and Alkoxy-Linked Pendant Amines **14i−bb**[a]
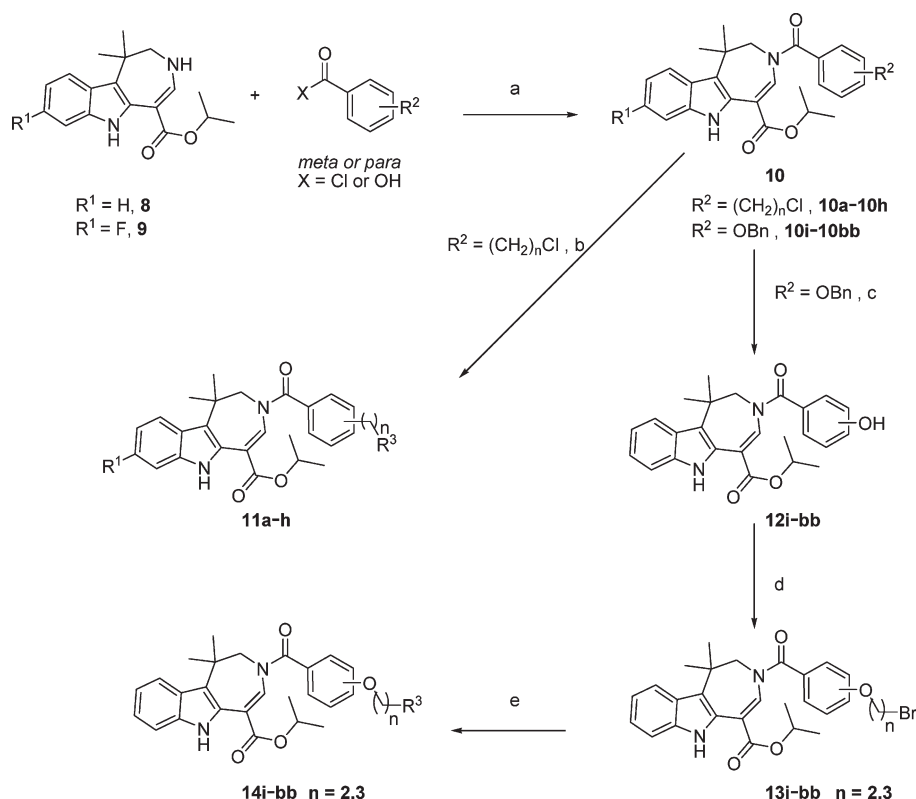

[a] Reagents: (a) acid chloride, TEA, CH₃CN, 0 °C to room temperature, 35−81%; or acid, TEA, EDC, dichloromethane, 30%; (b) TEA, requisite amine, CH₃CN, 0 °C to room temperature, 50−70%; or TEA, morpholine, KI, 60 °C, 60−70%; (c) 1,4-cyclohexadiene, 20% Pd(OH)₂/C, CH₃OH/ EtOAc, 64 °C, 67−72%; (d) bromoethanol or bromopropanol, Ph₃P, DEAD, THF, 38−82%; (e) requisite amine, 1-methyl-2-pyrrolidinone, 16−70%.

(**10i−10bb**) for eventual incorporation of the O-linked alkyl-bromide tether by the Mitsunobu reaction (**13i−13bb**). The final targets, **11a−h** and **14i−bb**, were obtained by nucleophilic displacement of the halides with the requisite amine.
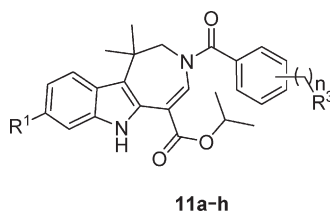
For key compounds, **14cc** and **14dd**, a large-scale alternative synthesis was developed with improved yields (Scheme 2). Benzyl-4-hydroxybenzoate was alkylated using a Mitsunobu reaction with the desired alcohol to provide **15cc−dd**, which were converted to the morpholine intermediates **16cc−dd**. Removal of the benzyl protecting group provided acids **17cc−dd**, which were converted to benzoyl chlorides. Subsequent treatment with isopropyl 8-fluoro-1,1-dimethyl-l,2,3,6-tetrahydroazepino[4,5-*b*]indole-5-carboxylate (**9**) provided **14cc** and **14dd** in 56−68% overall yields.

Results and Discussion

Compounds containing pendant amines were evaluated using an FXR functional assay to measure their ability to interact with the Gal4/human FXR-LBD in human embryonic kidney (HEK)293 cells. Maximal efficacy was reported as a percentage of the maximal efficacy observed for **2** in this assay. Additionally, compounds were profiled for microsomal stability[18] and solubility in 0.5% methylcellulose/2% Tween-80 in water (MC/T), the standard vehicle used for oral in vivo studies. A summary of data for all compounds prepared in Scheme 1 is displayed in Table 2 (compounds with carbon-linked pendant amines, **11a−h**) and Table 3 (compounds with alkoxy-linked pendant amines **14i−bb**). For the carbon-linked

Scheme 2. Scale-Up Procedure for the Preparation Multi-Gram Quantities of 8-Fluoro-azepino[4,5-*b*]indoles with Alkoxy-Linked Pendant Morpholines, **14cc** and **14dd**[a]
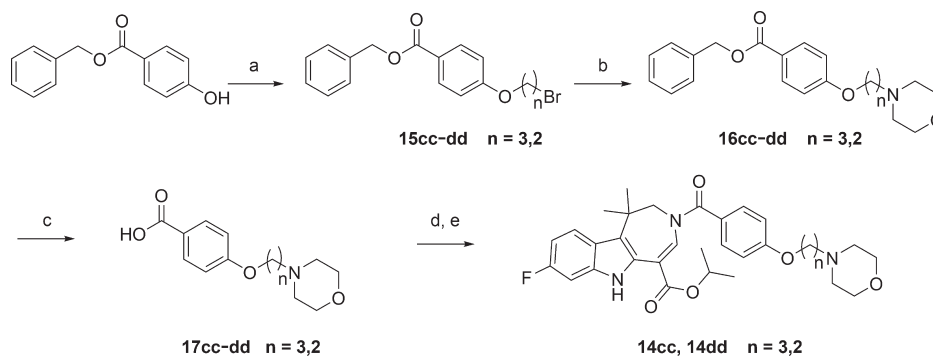
[a] Reagents: (a) bromoethanol or bromopropanol, THF, DIAD or DEAD, Ph$_3$P, 78−82%; (b) morpholine, CH$_3$CN, 97−100%; (c) 1,4-cyclohexadiene, 20% Pd(OH)$_2$/C, CH$_3$OH/EtOAc, 64 °C, 94−95%; (d) SOCl$_2$, 78 °C; (e) **9**, TEA, CH$_3$CN, 78−87%.

Table 2. Azepino[4,5-*b*]indoles with Carbon-Linked Pendant Amines, **11**

11a-h

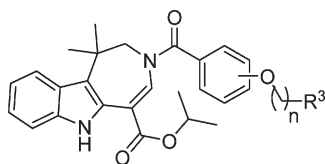| compound	R^1	n =	R^3	meta/para	hFXR EC$_{50}$[a] (nM)	efficacy in hFXR[b] (%)	stability (human)[d] $t_{(1/2)}$ min	stability (mouse)[d] $t_{(1/2)}$ min	MC/T solubility[e] (μg/mL)
11a	H	1	morpholine	meta	1579 ± 520	106 ± 6	5	4	ND[f]
11b	H	1	*N*-methyl piperazine	meta	368 ± 58	75 ± 4[c]	12	8	ND[f]
11c	H	1	piperidine	meta	534 ± 131	111 ± 21[c]	6	4	ND[f]
11d	H	1	pyrrolidine	meta	340 ± 46	90 ± 5[c]	ND[f]	ND[f]	ND[f]
11e	H	1	morpholine	para	23 ± 3	68 ± 14	15	2.5	245
11f	F	1	morpholine	para	447 ± 95	149 ± 5	>30	4	380
11g	H	2	morpholine	para	602 ± 131	143 ± 10	>30	2	4110[g]
11h	F	2	morpholine	para	342 ± 93	162 ± 8	26	5	5647[g]

[a] Induction of human FXR measured in HEK293 stable clones expressing Gal4/human FXR-LBD. [b] Efficacy = [maximal fold induction of test compound/maximal fold induction of compound **2** × 100]. [c] Indicates a decrease in efficacy at higher concentrations (>3 μM). [d] Liver microsomal. [e] Equilibrium solubility in 0.5% methylcellulose/2% Tween-80 in water. [f] ND: not determined. [g] Tested as the hydrochloride salt.

compounds in Table 2, **11e** (1-carbon para-linked morpholine), showed the best potency (EC$_{50}$ = 23 nM). The corresponding meta analogue (**11a**) and 8-fluoro version (**11f**) showed significantly less potency, but improved human liver microsome stability. Extending the linkage to 2-carbons also resulted in diminished potency in **11g** and **11h**. These two compounds were tested as the hydrochloride salts and showed very good solubility in the MC/T vehicle. Compound **11** (Table 2) or **14** (Table 3) containing more basic solubilizing groups (base pKas >8, that is, *N,N*-dimethylamine, pyrrolidine, piperidine, and *N*-methylpiperazine) than morpholine in Tables 2 and 3 all showed decreased efficacy at higher concentrations. For compounds in Table 3, meta-linked ether analogues with 2−3 carbon tethers were significantly weaker in potency (EC$_{50}$'s ≈ 1 μM) than para-linked counterparts. Focusing on para-linked ether analogues with full efficacy identified morpholines **14i** (EC$_{50}$ = 101 nM, efficacy = 156%) and **14m** (EC$_{50}$ = 249 nM, efficacy = 144%). These compounds were soluble in MC/T vehicle, at 200 μg/mL and 80 μg/mL, respectively, as free-bases. This was significantly superior to compound **1** (MC/T solubility 14 μg/mL), with the added possibility of salt formation to improve formulation properties. However, these compounds needed improvement in the area of microsome stability

profiling. For potential improvement in stability, the 8-fluoro analogues of **14i** and **14m** were prepared (Scheme 2, analogues **14cc** and **14dd**, respectively).
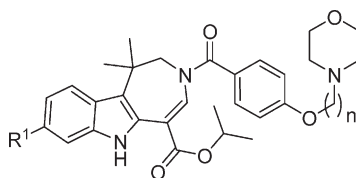
The FXR in vitro data and profiling data for these compounds are shown in Table 4 for comparison. The effect of incorporating a fluorine atom in the 8-position for **14cc** and **14dd** provided hFXR potency < 100 nM with full efficacy, which was equal or better than the *des*-fluoro analogues **14i** and **14m**. In the mFXR, **14cc** was the most potent compound (mFXR EC$_{50}$ = 52 nM, efficacy = 117%). The 8-fluoro functionality also decreased hERG binding and significantly improved microsomal stability for **14cc** when compared to the corresponding *des*-fluoro compound **14i**.

The pharmacokinetic parameters of **14cc** and **14dd** in male C57 Mouse and Sprague−Dawley rats are summarized in Table 5. In each species, the compounds showed high clearance and long terminal and elimination half-lives. Bioavailability (*F%*) for each compound was determined with dosing in MC/T. For **14cc**, bioavailability was moderate in the C57 mouse (*F* = 21%) and Sprague−Dawley rat (*F* = 38%). For **14dd**, bioavailability was good in the C57 mouse (*F* = 53%) and moderate in the Sprague−Dawley rat (*F* = 25%).

Table 3. Azepino[4,5-*b*]indoles with Alkoxy-Linked Pendant Amines, **14**

14i-bb

compound	R[1]	n =	R[3]	meta/para	hFXR EC$_{50}$[a] (nM)	efficacy in hFXR[b] (%)	stability (human)[d] $t_{(1/2)}$ min	stability (mouse)[d] $t_{(1/2)}$ min	MC/T solubility[e] (µg/mL)
14i	H	3	morpholine	para	101 ± 29	156 ± 12	15	8	200
14j	H	2	piperidine	para	1066 ± 129	140 ± 11[c]	14	9	80
14k	H	2	*N,N*-dimethylamine	para	439 ± 104	124 ± 13[c]	23	> 30	17
14l	H	2	pyrrolidine	para	698 ± 168	112 ± 8[c]	22	> 30	24
14m	H	2	morpholine	para	249 ± 70	144 ± 14	7	3	80
14n	H	2	*N*-methyl piperazine	para	287 ± 18	125 ± 11[c]	21	28	82
14o	H	3	*N,N*-dimethylamine	para	271 ± 20	106 ± 11[c]	15	23	2470
14p	H	3	pyrrolidine	para	362 ± 61	103 ± 3[c]	17	16	2330
14q	H	3	piperidine	para	424 ± 72	103 ± 8[c]	12	11	1220
14r	H	3	*N*-methyl piperazine	para	194 ± 17	128 ± 2[c]	18	11	1140
14s	H	2	*N,N*-dimethylamine	meta	1386 ± 356	88 ± 35[c]	8	8	536
14t	H	2	pyrrolidine	meta	1317 ± 343	99 ± 31[c]	ND[f]	ND[f]	ND[f]
14u	H	2	piperidine	meta	894 ± 242	98 ± 22[c]	5	5	111
14v	H	2	morpholine	meta	855 ± 220	119 ± 26	3	2	155
14w	H	2	*N*-methyl piperazine	meta	2870 ± 23	108 ± 25[c]	5	9	ND
14x	H	3	*N,N*-dimethylamine	meta	617 ± 17	76 ± 8[c]	> 30	> 30	ND
14y	H	3	pyrrolidine	meta	1603 ± 64	70 ± 18[c]	ND[f]	ND[f]	ND[f]
14z	H	3	piperidine	meta	1121 ± 76	69 ± 21[c]	5	11	1042
14aa	H	3	morpholine	meta	796 ± 207	127 ± 13	4	4	118
14bb	H	3	*N*-methyl piperazine	meta	1023 ± 69	90 ± 16[c]	6	12	1735

[a] Induction of human FXR measured in HEK293 stable clones expressing Gal4/human FXR-LBD. [b] Efficacy = [maximal fold induction of test compound/maximal fold induction of compound **2** × 100]. [c] Indicates a decrease in efficacy at higher concentrations (> 3 µM). [d] Liver microsomal. [e] Equilibrium solubility in 0.5% methylcellulose/2% Tween-80 in water. [f] ND: not determined.

Table 4. Comparison of Azepino[4,5-*b*]indoles Containing a para-Alkoxy-linked Morpholine

compound	R[1]	n	hFXR EC$_{50}$[a] (nM)	efficacy in hFXR[b] (%)	mFXR EC$_{50}$[c] (nM)	efficacy in mFXR[b] (%)	hERG IC$_{50}$ (µM)	stability (human)[d] $t_{(1/2)}$ min	stability (mouse)[d] $t_{(1/2)}$ min	MC/T solubility[e] (µg/mL)
14i	H	3	101 ± 29	156 ± 12	108 ± 5	87 ± 12	5.74	15	8	200
14m	H	2	249 ± 70	144 ± 14	190 ± 28	88 ± 19	19% @ 10 µM	7	3	80
14cc	F	3	88 ± 7	219 ± 40	52 ± 12	117 ± 18	> 30 µM	> 30	29	250; 5920[f]
14dd	F	2	99 ± 8	160 ± 23	188 ± 52	110 ± 20	> 30 µM	25	7	280; > 6000[f]
1	Figure 1		15 ± 6	141 ± 22	152 ± 86	174 ± 81	21% @ 10 µM	20	13.5	14

[a] Induction of human FXR measured in HEK293 stable clones expressing Gal4/human FXR-LBD. [b] Efficacy = [maximal fold induction of test compound/maximal fold induction of compound **2** × 100]. [c] Induction of mouse FXR measured in HEK293 stable clones expressing Gal4/mouse FXR-LBD. [d] Liver microsomal. [e] Equilibrium solubility in 0.5% methylcellulose/2% Tween-80 in water. [f] Tested as the hydrochloride salt.

To help determine how these compounds containing pendant solubilizing groups were acting as FXR agonists, the crystal structure of **14cc** bound to the LBD of human FXR was determined at a resolution of 1.9 Å (Figure 3). While the overall structure and the position of helix-12 were similar to that of previously disclosed X-ray structure of its close analogue, that is, compound **1**,[16] differences were observed in the loop region between helices 5 and 6. In addition, residues 268−282 of the helix-2 region were disordered in **14cc** and hence not resolved in the X-ray structure. As shown

in Figure 4, the **14cc** ligand resides in a predominantly hydrophobic pocket with the indoleazepine ring surrounded by residues Phe465, Trp458, Ile361, and Leu291. The carbonyl group of the amide makes hydrogen bond with the Tyr373 residue and is similar to that seen in X-ray structure of **1**. In addition, there is an internal hydrogen bond formed between the indole NH of the pyrrole and the ester carbonyl group which allows the template to rigidify further and orient the isopropyl ester group toward the narrow hydrophobic pocket surrounded by His298. The morpholine linker extends toward

Table 5. Pharmacokinetic Parameters of Compounds **14cc** and **14dd** after Intravenous and Oral Administrations in Male C57 Mice and Male Sprague-Dawley Rats[a]

species	dose (mg/kg)	compd	Cl ((mL/min)/kg)	C_{max} (ng/mL)	T_{max} (h)	$t_{1/2}$ (h)	AUC_{0-inf} (h ng/mL)	$F\%$
male C57 mouse	**3** (iv)	**14cc**	29			6.3	1722	
	3 (iv)	**14dd**	40			5.6	1256	
	3 (po)	**14cc**		81	1	6.4	370	21
	30 (po)	**14dd**		1127	1	5.5	6699	53
male Sprague−Dawley rat	**3** (iv)	**14cc**	52			6.3	960	
	3 (iv)	**14dd**	64			8	781	
	3 (po)	**14cc**		68	2	3.2	361	38
	3 (po)	**14dd**		35	1.7	4	193	25

[a] 0.5% methylcellulose/2% Tween-80 in water and 1-methyl-2-pyrrolidinone/PEG400/PG (10:40:50) were used as vehicles for oral and intravenious administrations, respectively. At least two animals were used in each study.
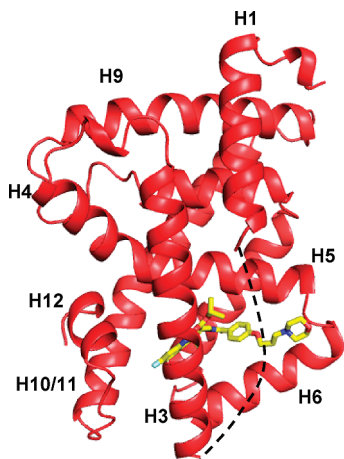
Figure 3. Overall structure of human FXR (red) in complex with **14cc** ligand (yellow). Helices are labeled as H1−H12. Helix-2 region which is disordered and missing in the structure is shown by dotted lines.
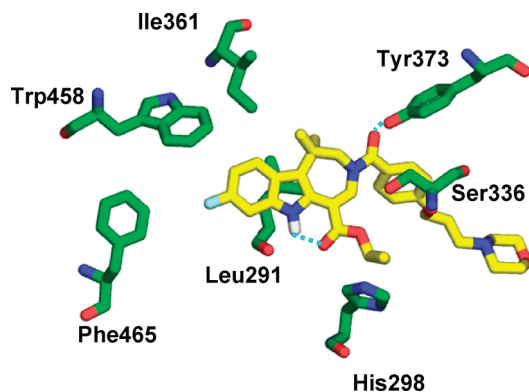
Figure 4. Specific interactions between **14cc** and critical residues in the FXR binding pocket. Hydrogen bonds are shown by cyan dotted line.

solvent and appears to use an induced fit mechanism to interact with FXR whereby the helix-2 undergoes a significant change in position in order to create room for this bulky group. This conclusion was reached from an overlay of the structure of compound **1** to the current structure which showed that this linker would sterically clash with helix-2 in the conformation observed for compound **1** complexed with the hFXR-LBD. We believe that the disorder in helix-2 region of the **14cc** structure is a direct effect of the shift in its position, which is made in order to accommodate the morpholine linker. Interestingly, as a result of these changes the loop

region between the helix-5 and helix-6 was also shifted toward the ligand in an effort to stabilize the linker. The structural plasticity of the FXR binding pocket further suggests that this receptor has the ability to accommodate different shaped ligands. In fact, the available FXR X-ray crystal structures clearly show that a wide range of diverse ligands are able to bind to this receptor by inducing conformational changes on the receptor. This receptor flexibility is a common theme among other nuclear receptor structures such as androgen receptor[19] and LXRβ[20] where side chain rearrangements in the ligand binding pocket allow ligands that differ in shape and size to bind with high affinity.

To determine the pharmacokinetic (PK) and pharmacodynamic (PD) relationship with **14cc** and **14dd**, LDL receptor knockout (LDLR$^{-/-}$) mice were treated orally with 3 mg/kg of each compound in MC/T and blood and liver samples were harvested over a 24 h period. Interestingly, the extent of the induction of hepatic SHP (short heterodimer partner) correlated with the changes in systemic exposure over time (Figure 5A,B).

Significant modulation of serum lipoproteins was also observed in the LDLR$^{-/-}$ model of dyslipidemia. Male LDLR$^{-/-}$ mice were placed onto a Western diet and treated for 7 days orally with varying concentrations of either compound. As shown in Figure 6 both **14cc** and **14dd** significantly lowered in serum LDLc levels as well as serum TG and cholesterol levels (data not shown) consistent with previous observations.[12]

Because of the improved PK properties, the ability of **14cc** to regulate lipoprotein metabolism was tested in rhesus monkeys, since primates are thought to be most representative of human physiology. Female rhesus monkeys on a standard diet were treated daily orally with MC/T vehicle or 60 mg/kg **14cc** over 4 weeks. As anticipated, **14cc** treatment resulted in a significant decrease in TG and VLDLc levels after 7 days of treatment (Figure 7A,B) even though these monkeys were not considered dyslipidemic. Interestingly, pronounced LDLc lowering (63%) was also observed with no effect on HDLc levels (Figure 7C,D). These effects were maximal after 7 days and were maintained over the course of the study.

Importantly, the lowering of serum cholesterol and TG levels was not due to hepatic lipid accumulation with no significant difference in either between the control and treated monkeys (data not shown). To begin to address the mechanism for the reduction in LDL, hepatic regulation of genes involved in lipid metabolism was monitored. As shown in Figure 8, LDLR expression was significantly induced by **14cc** treatment. This induction in LDLR mRNA is consistent with the induction observed in human hepatocytes, which was demonstrated to be mediated via a FXR-dependent reduction
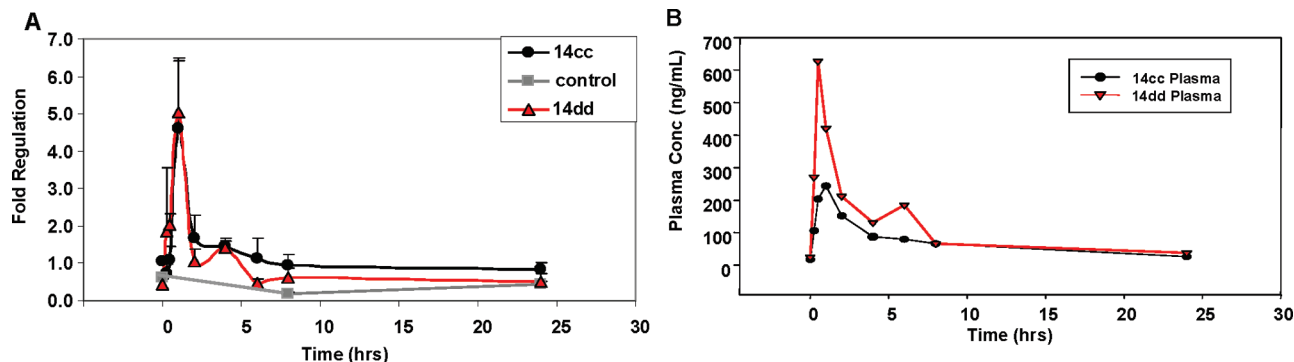
Figure 5. The establishment of PK and PD relationship with **14cc** and **14dd**. (A) LDLR$^{-/-}$ mice were treated with MC/T vehicle (control) or 3 mg/kg **14cc** or **14dd**. The livers were harvested at varying time points for RNA analysis of SHP gene expression. (B) Blood samples were collected at the same time points for determination of plasma concentrations.
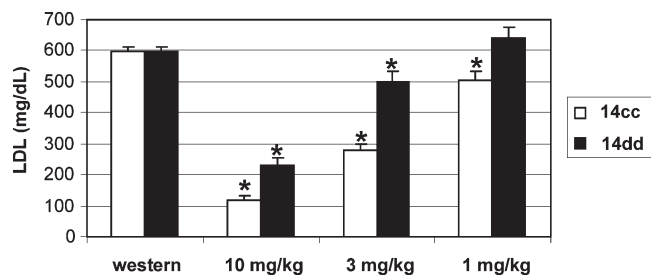

Figure 6. Regulation of LDL lipoprotein fraction in LDLR$^{-/-}$ mice. *S*erum LDLc, levels were determined by FPLC from male LDLR$^{-/-}$ mice treated orally for 7 days with increasing concentrations of either **14cc** or **14dd** as indicated and expressed as mg/dL. *$P < 0.01$ vs western diet-fed control mice.

in PCSK9 expression.[21] An additional pathway that may be contributing to LDL levels could be the bile acid synthetic pathway which results in the catabolism of hepatic cholesterol. As shown in Figure 8, cyp7a1 mRNA levels are dramatically inhibited by **14cc** treatment as expected. However, no regulation of cyp8b1 expression was observed. It was previously shown that cyp8b1 gene expression is repressed by FXR agonists in mice while induced in humans,[22] suggesting that the composition of the bile acid pool, the rate of cholesterol catabolism, and its impact on intestinal cholesterol absorption may be distinct in these three species in the presence of a FXR agonist. Overall, these data are the first to demonstrate the dramatic lowering of serum LDL levels by a FXR agonist in primates and supports the potential utility of **14cc** in treating dyslipidemia in humans beyond just TG lowering.

Conclusion

The focus of this work centered around enhancing the formulation properties of FXR agonists containing the azepino[4,5-*b*] core. Crystallography data for lead compound **1** showed that solubilizing groups might be tolerated if they were tethered away from the lipophilic FXR-LBD, toward surrounding solvent. To explore this strategy, we developed chemistry to incorporate pendant solubilizing amines tethered from the benzoyl functionality. Our approach systematically explored positioning (meta or para) and length of the tether, in combination with amines offering a range of basicity. For compounds with the 1−2 carbon tether **11** (Table 2), the para-linked pendant morpholines (**11e**−**11h**) provided moderate hFXR potency and good efficacy. For the alkoxy-linked

pendant amines **14** (Table 3), the para-linked pendant morpholines **14i** and **14m** possessed potency of 101 nM and 249 nM, respectively, with full efficacy. The corresponding meta-analogues were significantly less potent, as well as compounds with more basic pendant amines than morpholine, which displayed decreased efficacy at concentrations > 3 μM. To improve microsome stability of **14i** and **14m**, the 8-fluoro analogues **14cc** and **14dd** were prepared, respectively. In comparison to **1**, these compounds demonstrated a 6-fold decrease in hFXR potency, but realized markedly better solubility in MC/T, the standard vehicle used for oral in vivo studies. In fact, the solubility for each compound was improved even more dramatically through formulation as the hydrochloride salts (Table 4, MC/T solubility). The X-ray crystal structure of **14cc** shows that the pendant morpholine appears to reach the solvent cavity past helix-2, as we had hoped. Helix-2 apparently shifts to accommodate the bulky solubilizing functionality. Analysis in vivo revealed full FXR agonist activity. In LDLR$^{-/-}$ mice, **14cc** and **14dd** in MC/T, reduced LDLc in a dose-dependent fashion. Additionally, SHP gene expression in the LDLR$^{-/-}$ mouse correlated well with blood levels over time. In female rhesus monkeys, dosing with **14cc** in MC/T at 60 mg/kg daily for 4 weeks resulted in a significant lowering of TG, VLDLc, and LDLc. The ability to dose the FXR agonist, **14cc**, in a pharmaceutically acceptable vehicle may prove useful for treatment of dyslipidemia in humans.

Experimental Section

General. Solvents and chemicals were purchased from EM Sciences, VWR, and Aldrich Chemical Co. and used without further purification. ^{1}H NMR spectra were recorded on a Varian INOVA 400 instrument, and chemical shifts are reported in δ values (parts per million, ppm) relative to an internal standard tetramethylsilane in CDCl$_3$ or DMSO-d_6. Abbreviations for NMR multiplets are as follows: br s − broad singlet, s − singlet, d − doublet, t − triplet, q − quartet, quin − quintet. Electrospray (ESI) mass spectra were recorded using a Waters Alliance-ZMD mass spectrometer. Electron impact ionization (EI, EE = 70 eV) mass spectra were recorded on a Finnigan Trace mass spectrometer. Analytical thin layer chromatography (TLC) was performed on precoated plates (silica gel, 60 F-254) and was visualized using UV light and/or staining with a phosphomolybdic acid solution in ethanol. In general, purity for key compounds was confirmed at ≥95% using the following analytical HPLC method: photodiode array detection was between 210−400 nm; the LC was performed on an Agilent 1100 HPLC using a Waters Xterra RP18 HPLC column (150 mm × 4.6 mm ID, 3.5 μ), 40 °C column oven
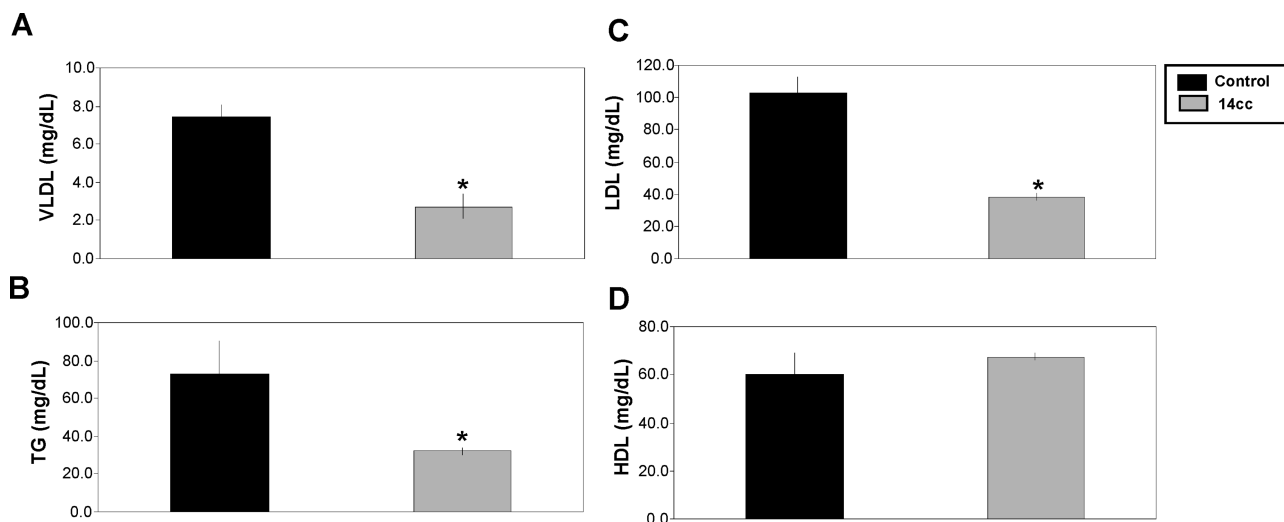
A

B

C

D

Figure 7. Regulation of lipoprotein fractions in rhesus monkeys. Serum (A) VLDLc, (C) LDLc, and (D) HDLc levels were determined by FPLC, while (B) TG levels were determined using a clinical analyzer and all are expressed as mg/dL. *$P < 0.05$ vs MC/T vehicle control monkeys.
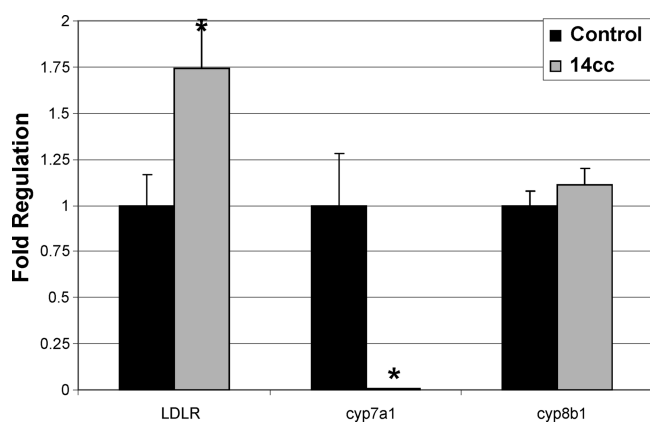

Figure 8. Regulation of hepatic gene expression by **14cc** treatment for 28 days. Hepatic expression of LDLR, cyp7a1, and cyp8b1 levels from female rhesus monkeys described in Figure 7 were determined by real-time RT-PCR and normalized to 18S. *$P < 0.01$ vs MC/T control monkeys.

temperature, 1.2 mL/min flow rate, linear mobile phase gradient of 15 to 95% B over 10 min, holding 5 min at 95% B (mobile phase A: 10 mM ammonium formate in water, pH 3.5; mobile phase B: 1:1 methanol/acetonitrile). The analytical HPLC results using this method are provided as retention time (R_t) and purity (%) for each compound tested in biological assays.

General Procedure for the Acylation of Indoleazepines 10i−bb. A solution of isopropyl-1,1-dimethyl-1,2,3,6-tetrahydroazepino-[4,5-*b*]indole-5-carboxylate, (**8**) (1.2 g, 4 mmol) in dry acetonitrile (20 mL) and TEA (837 μL, 6 mmol) was added to a solution of the appropriate benzoyl chloride (6 mmol) in dry acetonitrile (15 mL). The reaction mixture was stirred for 1 h at room temperature after which distilled water (40 mL) was added. The resulting precipitate was collected by vacuum filtration and recrystallized from EtOAc/hexane (5:1, 12 mL) to provide the desired product (**10i−bb**) (35−81% yields).

Isopropyl 3-[4-(Benzyloxy)benzoyl]-1,1-dimethyl-1,2,3,6-tetra-hydroazepino[4,5-*b*]indole-5-carboxylate 10i−r. ^{1}H NMR (400 MHz, DMSO-d_6) δ 10.83 (s, 1H), 7.75 (d, $J = 8.2$ Hz, 1H), 7.73 (s, 1H), 7.56−7.53 (m, 1H), 7.52 (d, $J = 9.0$ Hz, 2H), 7.47−7.30 (m, 5H), 7.13 (d, $J = 9.0$ Hz, 2H), 7.10−7.05 (m, 1H), 7.01−6.95 (m, 1H), 5.20 (s, 2H), 5.04 (quin, $J = 6.2$ Hz, 1H), 3.97 (br s, 2H), 1.51 (s, 6H), 1.16 (d, $J = 6.2$ Hz, 6H); MS (ES, [M + H]$^+$), m/z 509.0.

Isopropyl 3-[3-(Benzyloxy)benzoyl]-1,1-dimethyl-1,2,3,6-tetra-hydroazepino[4,5-*b*]indole-5-carboxylate 10s−bb. ^{1}H NMR (400 MHz, DMSO-d_6) δ 10.83 (s, 1H), 7.76 (d, $J = 8.2$ Hz, 1H), 7.69 (s, 1H), 7.55 (d, $J = 8.2$ Hz, 1H), 7.46−7.37 (m, 3H), 7.34−7.28 (m, 3H), 7.25 (ddd, $J = 1.0, 2.5, 8.4$ Hz, 1H), 7.16−7.13 (m, 1H), 7.11−7.05 (m, 2H), 6.98 (ddd, $J = 1.0, 7.0, 8.0$ Hz, 1H), 5.14 (s, 2H), 5.03 (quin, $J = 6.2$ Hz, 1H), 3.95 (br. s., 2H), 1.50 (s, 6H), 1.15 (d, $J = 6.2$ Hz, 6H); HRMS: calcd for $C_{32}H_{32}N_2O_4 + H^+$, 509.2435; found (ESI, [M + H]$^+$), 509.2438.

General Procedure for the Acylation of Indoleazepines 10a−f. A solution of the appropriately substituted indoleazepine (**8** or **9**) (1.0 mmol) in dry acetonitrile (15 mL) under nitrogen was cooled to 0 °C. To this solution was added TEA (0.17 mL, 1.2 mmol) and the appropriately substituted-(chloromethyl)-benzoyl chloride (1.5 mmol). The reaction mixture was stirred at room temperature for 3 h. The mixture was filtered and the filtrate was concentrated under reduced pressure. The resulting crude product was purified via Isco (RediSep Flash Column 12 g, silica, CH$_2$Cl$_2$/hexane 20:80−100:0) to give the expected product. The crude material was recrystallized from hexane/isopropyl alcohol to afford the desired product (**10a−f**) (35−81% yields).

Isopropyl 3-(3-(Chloromethyl)benzoyl)-1,1-dimethyl-1,2,3,6-tetrahydroazepino[4,5-*b*]indole-5-carboxylate 10a−d. ^{1}H NMR (400 MHz, DMSO-d_6) δ 10.86 (s, 1H), 7.77 (d, $J = 8.2$ Hz, 1H), 7.67−7.65 (m, 1H), 7.68 (dd, $J = 1.5, 2.8$ Hz, 1H), 7.63−7.60 (m, 1H), 7.56 (s, 1H), 7.56−7.53 (m, 2H), 7.08 (ddd, $J = 1.0, 7.0, 8.1$ Hz, 1H), 6.98 (ddd, $J = 1.0, 7.0, 8.1$ Hz, 1H), 5.02 (quin, $J = 6.2$ Hz, 1H), 4.82 (s, 2H), 3.99 (br s, 2H), 1.53 (s, 6H), 1.14 (d, $J = 6.2$ Hz, 6H); HRMS: calcd for $C_{26}H_{27}ClN_2O_3 + H^+$, 451.1783; found (ESI, [M + H]$^+$), 451.1785.

Isopropyl 3-(4-(Chloromethyl)benzoyl)-1,1-dimethyl-1,2,3,6-tetrahydroazepino[4,5-*b*]indole-5-carboxylate 10e. ^{1}H NMR (400 MHz, DMSO-d_6) δ 10.83 (s, 1H), 7.76 (d, $J = 8.0$ Hz, 1H), 7.65 (s, 1H), 7.58−7.55 (m, 5H), 7.08 (t, $J = 7.4$ Hz, 1H), 6.98 (t, $J = 7.4$ Hz, 1H), 5.02 (quin, $J = 6.2$ Hz, 1H), 4.83 (s, 2H), 3.97 (br s, 2H), 1.53 (s, 6H), 1.14 (d, $J = 6.2$ Hz, 6H); MS (ES, [M + H]$^+$), m/z 451.1.

Isopropyl 3-[4-(Chloromethyl)benzoyl]-8-fluoro-1,1-dimethyl-1,2,3,6-tetrahydroazepino[4,5-*b*]indole-5-carboxylate 10f. ^{1}H NMR (400 MHz, DMSO-d_6) δ 10.98 (s, 1H), 7.76 (dd, $J = 5.5, 9.0$ Hz, 1H), 7.66 (s, 1H), 7.60−7.53 (m, 4H), 7.36 (dd, $J = 2.5, 10.0$ Hz, 1H), 6.83 (ddd, $J = 1.1, 7.0, 8.0$ Hz, 1H), 5.01 (quin, $J = 6.2$ Hz, 1H), 4.83 (s, 2H), 3.96 (br s, 2H), 1.51 (s, 6H), 1.13 (d, $J = 6.2$ Hz, 6H); MS (ES, [M + H]$^+$), m/z 469.0.

General Procedure for the Acylation of Indoleazepines 10g−h. A solution of the appropriately substituted indoleazepine (**8** or **9**)

(1.5 mmol) in dry CH_2Cl_2 (20 mL) under nitrogen was treated with TEA (0.21 mL, 1.8 mmol). To this solution was added 1-ethyl-3-(3-dimethylaminopropyl) carbodiimide hydrochloride (EDC) (0.52 g, 1.8 mmol) and 4-(2-chloroethyl)benzoic acid (0.33 g, 1.8 mmol) and the reaction mixture was stirred at room temperature for 3 days. The mixture was then washed with water, dried over anhydrous sodium sulfate, filtered, and concentrated under reduced pressure. The resulting residue was purified via lsco (RediSep Flash Column 12 g, silica, EtOAc/hexane 5:95−20:80) followed by recrystallization from EtOAc/hexane to give the desired product (**10g−h**) (30% yields).

Isopropyl 3-[4-(2-Chloroethyl)benzoyl]-1,1-dimethyl-1,2,3,6-tetrahydroazepino[4,5-*b*]indole-5-carboxylate 10g. ^{1}H NMR (400 MHz, DMSO-d_6) δ 10.84 (s, 1H), 7.76 (d, $J = 8.0$ Hz, 1H), 7.69 (s, 1H), 7.55 (ddd, $J = 1.0, 1.0, 8.0$ Hz, 1H), 7.49 (d, $J = 8.3$ Hz, 2H), 7.43 (d, $J = 8.3$ Hz, 2H), 7.08 (ddd, $J = 1.0, 7.0, 8.0$ Hz, 1H), 6.98 (ddd, $J = 1.0, 7.0, 8.0$ Hz, 1H), 5.02 (quin, $J = 6.2$ Hz, 1H), 3.97 (br s, 2H), 3.89 (t, $J = 6.7$ Hz, 2H), 3.11 (t, $J = 6.7$ Hz, 2H), 1.53 (s, 6H), 1.14 (d, $J = 6.2$ Hz, 6H); HRMS: calcd for $C_{27}H_{29}ClN_2O_3 + H^+$, 465.1939; found (ESI, [M + H]$^+$), 465.1939.

Isopropyl 3-(4-(2-Chloroethyl)benzoyl)-8-fluoro-1,1-dimethyl-1,2,3,6-tetrahydroazepino[4,5-*b*]indole-5-carboxylate 10h. ^{1}H NMR (400 MHz, DMSO-d_6) δ 10.98 (s, 1H), 7.76 (dd, $J = 5.4, 9.0$ Hz, 1H), 7.69 (s, 1H), 7.49 (d, $J = 8.2$ Hz, 2H), 7.43 (d, $J = 8.2$ Hz, 2H), 7.36 (dd, $J = 2.5, 10.2$ Hz, 1H), 6.83 (ddd, $J = 2.5, 9.2, 9.2$ Hz, 1H), 5.01 (quin, $J = 6.3$ Hz, 1H), 3.96 (br. s., 2H), 3.89 (t, $J = 6.7$ Hz, 2H), 3.11 (t, $J = 6.7$ Hz, 2H), 1.51 (s, 6H), 1.13 (d, $J = 6.2$ Hz, 6H); HRMS: calcd for $C_{27}H_{28}ClFN_2O_3 + H^+$, 483.1845; found (ESI, [M + H]$^+$), 483.1844.

General Procedure for the Synthesis of Carbon-Tethered Amines 11a−f. A solution of alkyl chloride (**10a−f**) (0.22 mmol) and TEA (0.036 mL, 0.26 mmol) in dry acetonitrile (5 mL) was stirred at 0 °C. To this solution was added the appropriate amine (0.33 mmol) and the reaction mixture was stirred at room temperature for 15 h. The reaction mixture was then partitioned between a saturated aqueous solution of sodium bicarbonate and CH_2Cl_2. The separated CH_2Cl_2 layer was washed with water, dried over anhydrous sodium sulfate, filtered, and concentrated under reduced pressure. The resulting crude product was purified via Isco (RediSep Flash Column 12 g, silica, EtOAc/hexane 0:100−100:0) to yield the expected product (**11a−f**) (50−70% yields).

Isopropyl 1,1-Dimethyl-3-[3-(morpholin-4-ylmethyl)benzoyl]-1,2,3,6-tetrahydroazepino[4,5-*b*]indole-5-carboxylate 11a. ^{1}H NMR (400 MHz, DMSO-d_6) δ 10.85 (s, 1H), 7.77 (d, $J = 8.2$ Hz, 1H), 7.61 (s, 1H), 7.56 (d, $J = 8.0$ Hz, 1H), 7.54−7.52 (m, 1H), 7.48 (t, $J = 7.43$ Hz, 1H), 7.46−7.43 (m, 1H), 7.42 (s, 1H), 7.08 (ddd, $J = 1.0, 7.0, 8.1$ Hz, 1H), 6.98 (ddd, $J = 1.0, 7.0, 8.1$ Hz, 1H), 4.99 (quin, $J = 6.2$ Hz, 1H), 3.97 (br s, 2H), 3.55−3.48 (m, 6H), 3.29 (s, 2H), 2.36−2.31 (m, 4H), 1.53 (s, 6H), 1.12 (d, $J = 6.2$ Hz, 6H); HRMS: calcd for $C_{30}H_{35}N_3O_4 + H^+$, 502.2700; found (ESI, [M + H]$^+$), 502.2696; Analytical HPLC: $R_t = 10.9$ min (100%).

Isopropyl 1,1-Dimethyl-3-{3-[(4-methylpiperazin-1-yl)methyl]benzoyl}-1,2,3,6-tetrahydroazepino[4,5-*b*]indole-5-carboxylate 11b. ^{1}H NMR (400 MHz, CDCl$_3$) δ 10.70 (s, 1H), 7.83 (d, $J = 8.2$ Hz, 1H), 7.80 (s, 1H), 7.54 (s, 1H), 7.49 (d, $J = 7.4$ Hz, 1H), 7.45−7.41 (m, 1H), 7.38 (d, $J = 7.7$ Hz, 2H), 7.18 (ddd, $J = 1.0, 7.0, 8.1$ Hz, 1H), 7.08 (ddd, $J = 1.0, 7.0, 8.1$ Hz, 1H), 5.10 (quin, $J = 6.2$ Hz, 1H), 4.07 (br s, 2H), 3.53 (s, 2H), 2.47 (br s, 8H), 2.27 (s, 3H), 1.64 (s, 6H), 1.16 (d, $J = 6.2$ Hz, 6H); HRMS: calcd for $C_{31}H_{38}N_4O_3 + H^+$, 515.3017; found (ESI, [M + H]$^+$), 515.3019; Analytical HPLC: $R_t = 10.0$ min (91.9%).

Isopropyl 1,1-Dimethyl-3-[3-(piperidin-1-ylmethyl)benzoyl]-1,2,3,6-tetrahydroazepino[4,5-*b*]indole-5-carboxylate 11c. ^{1}H NMR (400 MHz, CDCl$_3$) δ 10.72 (s, 1H), 7.83 (d, $J = 8.2$ Hz, 1H), 7.81 (s, 1H), 7.53−7.50 (m, 2H), 7.38−7.45 (m, 3H), 7.18 (ddd, $J = 1.1, 7.0, 8.1$ Hz, 1H), 7.08 (ddd, $J = 1.1, 7.0, 8.1$ Hz, 1H), 5.09 (quin, $J = 6.2$ Hz, 1H), 4.08 (br s, 2H), 3.49 (s, 2H),

2.36 (br s, 4H), 1.64 (s, 6H), 1.54 (quin, $J = 5.5$ Hz, 4H), 1.46−1.35 (m, 2H), 1.16 (d, $J = 6.2$ Hz, 6H); HRMS: calcd for $C_{31}H_{37}N_3O_3 + H^+$, 500.2908; found (ESI, [M + H]$^+$), 500.2913; Analytical HPLC: $R_t = 9.9$ min. (98.3%).

Isopropyl 1,1-Dimethyl-3-[3-(pyrrolidin-1-ylmethyl)benzoyl]-1,2,3,6-tetrahydroazepino[4,5-*b*]indole-5-carboxylate 11d. ^{1}H NMR (400 MHz, CDCl$_3$) δ 10.72 (s, 1H), 7.83 (d, $J = 8.2$ Hz, 1H), 7.80 (s, 1H), 7.56−7.48 (m, 2H), 7.38−7.46 (m, 3H), 7.18 (ddd, $J = 1.0, 7.0, 8.1$ Hz, 1H), 7.08 (ddd, $J = 1.0, 7.00, 8.1$ Hz, 1H), 5.09 (quin, $J = 6.2$ Hz, 1H), 4.08 (br s, 2H), 3.63 (s, 2H), 2.53−2.43 (m, 4H), 1.79−1.74 (m, 4H), 1.59 (br s, 6H), 1.16 (d, $J = 6.2$ Hz, 6H); HRMS: calcd for $C_{30}H_{35}N_3O_3 + H^+$, 486.2751; found (ESI, [M + H]$^+$), 486.2755; Analytical HPLC: $R_t = 9.7$ min. (96.6%).

Isopropyl 1,1-Dimethyl-3-[4-(morpholin-4-ylmethyl)benzoyl]-1,2,3,6-tetrahydroazepino[4,5-*b*]indole-5-carboxylate 11e. ^{1}H NMR (400 MHz, DMSO-d_6) δ 10.85 (s, 1H), 7.76 (d, $J = 8.2$ Hz, 1H), 7.68 (s, 1H), 7.55 (d, $J = 8.0$ Hz, 1H), 7.50 (d, $J = 8.2$ Hz, 2H), 7.45 (d, $J = 8.2$ Hz, 2H), 7.08 (ddd, $J = 1.1, 7.0, 8.0$ Hz, 1H), 6.98 (ddd, $J = 1.1, 7.0, 8.0$ Hz, 1H), 5.01 (quin, $J = 6.2$ Hz, 1H), 3.98 (br s, 2H), 3.60−3.55 (m, 4H), 3.53 (s, 2H), 2.39−2.31 (m, 4H), 1.53 (s, 6H), 1.11 (d, $J = 6.2$ Hz, 6H); HRMS: calcd for $C_{30}H_{35}N_3O_4 + H^+$, 502.2700; found (ESI, [M + H]$^+$), 502.2704; Analytical HPLC: $R_t = 11.0$ min (97.1%).

Isopropyl 8-Fluoro-1,1-dimethyl-3-[4-(morpholin-4-ylmethyl)benzoyl]-1,2,3,6-tetrahydroazepino[4,5-*b*]indole-5-carboxylate 11f. ^{1}H NMR (400 MHz, DMSO-d_6) δ 10.99 (s, 1H), 7.76 (dd, $J = 5.5, 9.0$ Hz, 1H), 7.69 (s, 1H), 7.51 (d, $J = 8.3$ Hz, 2H), 7.45 (d, $J = 8.3$ Hz, 2H), 7.36 (dd, $J = 2.5, 10.0$ Hz, 1H), 6.83 (ddd, $J = 2.5, 9.3, 9.3$ Hz, 1H), 5.01 (quin, $J = 6.2$ Hz, 1H), 3.96 (br s, 2H), 3.57 (d, $J = 4.5$ Hz, 4H), 3.53 (s, 2H), 2.35 (d, $J = 4.5$ Hz, 4H), 1.51 (s, 6H), 1.11 (d, $J = 6.2$ Hz, 6H); HRMS: calcd for $C_{30}H_{34}FN_3O_4 + H^+$, 520.2606; found (ESI, [M+H]$^+$), 520.2610; Analytical HPLC: $R_t = 11.1$ min (99.5%).

General Procedure for the Synthesis of Carbon-Tethered Amines 11g−h. To a solution of alkyl chloride (**10g−h**) (0.22 mmol) and morpholine (1.0 mL, 11 mmol) was added potassium iodide (0.037 g, 0.22 mmol) and TEA (0.035 mL, 0.26 mmol). The reaction mixture was stirred at 60 °C for 24 h and cooled to room temperature. The cooled mixture was partitioned between a saturated aqueous solution of sodium bicarbonate and CH_2Cl_2. The separated CH_2Cl_2 layer was washed with water, dried over anhydrous sodium sulfate, filtered, and concentrated under reduced pressure. The resulting crude product was purified via Isco (RediSep Flash Column 12 g, silica, methanol/CH_2Cl_2 0.125:99.875−1.25:98.75) to give the expected product (60−70% yields).

Preparation of Hydrochloride Salts. The HCl salts were formed by dissolving the product in a minimum amount of EtOAc, followed by treatment with hydrochloric acid (4 M in dioxane) to pH 3, followed by EtOAc to afford the final product (**11g−h**).

Isopropyl 1,1-Dimethyl-3-[4-(2-morpholin-4-ylethyl)benzoyl]-1,2,3,6-tetrahydroazepino[4,5-*b*]indole-5-carboxylate Hydrochloride 11g. ^{1}H NMR (400 MHz, DMSO-d_6) δ 10.82 (s, 1H), 7.76 (d, $J = 8.0$ Hz, 1H), 7.67 (s, 1H), 7.57−7.51 (m, 3H), 7.43 (d, $J = 8.2$ Hz, 2H), 7.08 (ddd, $J = 1.0, 7.0, 8.1$ Hz, 1H), 6.98 (ddd, $J = 1.0, 7.0, 8.1$ Hz, 1H), 5.03 (quin, $J = 6.2$ Hz, 1H), 4.04−3.94 (m, 4H), 3.76 (t, $J = 12.0$ Hz, 2H), 3.53−3.46 (m, 2H), 3.36 (br s, 2H), 3.18−3.04 (m, 4H), 1.52 (s, 6H), 1.17 (d, $J = 6.2$ Hz, 6H); HRMS: calcd for $C_{31}H_{37}N_3O_4 + H^+$, 516.2857; found (ESI, [M + H]$^+$), 516.2861; Analytical HPLC: $R_t = 9.9$ min. (100%).

Isopropyl 8-Fluoro-1,1-dimethyl-3-[4-(2-morpholin-4-ylethyl)benzoyl]-1,2,3,6-tetrahydroazepino[4,5-*b*]indole-5-carboxylate Hydrochloride 11h. ^{1}H NMR (400 MHz, DMSO-d_6) δ 10.97 (s, 1H), 7.76 (dd, $J = 5.4, 9.0$ Hz, 1H), 7.68 (s, 1H), 7.54 (d, $J = 8.2$ Hz, 2H), 7.43 (d, $J = 8.2$ Hz, 2H), 7.36 (dd, $J = 2.5, 10.0$ Hz, 1H), 6.84 (ddd, $J = 2.5, 9.2, 9.2$ Hz, 1H), 5.02 (quin, $J = 6.2$ Hz, 1H), 4.03−3.96 (m, 4H), 3.77 (t, $J = 12.0$ Hz, 2H),

3.53−3.46 (m, 2H), 3.36 (br s, 2H), 3.18−3.04 (m, 4H), 1.50 (s, 6H), 1.16 (d, J = 6.2 Hz, 6H); MS (ES, [M + H]$^+$), m/z 534.3; Analytical HPLC: R_t = 10.1 min (98.5%).

General Procedure for Benzyl Deprotection 12i−bb. A solution of benzyl esters (**10i−bb**) (393 μmol) in a mixture of methanol (9 mL) and EtOAc (1 mL) was stirred under nitrogen. To this solution was added 1,4-cyclohexadiene (375 μL, 3.93 mmol) and palladium hydroxide (20% on carbon, 100 mg) under nitrogen and the mixture was capped in a sealed tube. The reaction was stirred at 64 °C for 1−2 h. The reaction was cooled to room temperature and filtered through Celite. The Celite was rinsed with methanol (3 × 10 mL) and the combined filtrate was concentrated. The crude mixture was treated with diethyl ether/hexane (1:1, 3 mL) to provide the product (**12i−bb**) (67−72% yields).

Isopropyl 3-(4-Hydroxybenzoyl)-1,1-dimethyl-1,2,3,6-tetrahydroazepino[4,5-*b*]indole-5-carboxylate 12i−r. ^{1}H NMR (400 MHz, DMSO-d_6) δ 10.84 (s, 1H), 10.29 (br s, 1H), 7.78 (s, 1H), 7.75 (d, J = 8.1 Hz, 1H), 7.55 (d, J = 8.1 Hz, 1H), 7.43 (d, J = 8.8 Hz, 2H), 7.07 (ddd, J = 1.0, 7.0, 8.1 Hz, 1H), 6.97 (ddd, J = 1.0, 7.0, 8.1 Hz, 1H), 6.85 (d, J = 8.6 Hz, 2H), 5.05 (quin, J = 6.2 Hz, 1H), 3.96 (br s, 2H), 1.50 (s, 6H), 1.18 (d, J = 6.2 Hz, 6H); HRMS: calcd for $C_{25}H_{26}N_2O_4$ + H$^+$, 419.1965; found (ESI, [M + H]$^+$), 419.1970.

Isopropyl 3-(3-Hydroxybenzoyl)-1,1-dimethyl-1,2,3,6-tetrahydroazepino[4,5-*b*]indole-5-carboxylate 12s−bb. ^{1}H NMR (400 MHz, DMSO-d_6) δ 10.84 (s, 1H), 9.84 (br s, 1H), 7.76 (d, J = 7.7 Hz, 1H), 7.71 (s, 1H), 7.55 (d, J = 8.2 Hz, 1H), 7.31 (t, J = 8.2 Hz, 1H), 7.08 (ddd, J = 1.0, 7.6 Hz, 1H), 7.00−6.95 (m, 2H), 6.94−6.90 (m, 2H), 5.03 (quin, J = 6.2 Hz, 1H), 3.96 (br s, 2H), 1.52 (s, 6H), 1.16 (d, J = 6.2 Hz, 6H); HRMS: calcd for $C_{25}H_{26}N_2O_4$ + H$^+$, 419.1965; found (ESI, [M + H]$^+$), 419.1965.

General Procedure for Ether Formation 13i−bb. To a solution of the appropriate phenol (**12i−bb**) (191 μmol) in THF (2 mL) was added either bromoethanol or bromopropanol (348 μmol), triphenylphosphine (91.3 mg, 348 μmol), and DEAD (54.1 μL, 344 μmol). The reaction was stirred under nitrogen at room temperature for 18 h. The crude reaction was concentrated under reduced pressure and diluted with diethyl ether (10 mL) and washed with water (3 × 10 mL). The organic layer was dried over magnesium sulfate, filtered, and concentrated under reduced pressure. The resulting residue was purified via Isco (RediSep Flash Column 12 g, silica, EtOAc/hexane 5:95−25:75) to give the desired product (**13i−bb**) (38−82% yields).

Isopropyl 3-[4-(3-Bromopropoxy)benzoyl]-1,1-dimethyl-1,2,3,6-tetrahydroazepino[4,5-*b*]indole-5-carboxylate 13i, 13o−r. ^{1}H NMR (400 MHz, DMSO-d_6) δ 10.84 (s, 1H), 7.78−7.73 (m, 2H), 7.55 (d, J = 8.0 Hz, 1H), 7.52 (d, J = 8.8 Hz, 2H), 7.10−7.05 (m, 3H), 6.98 (ddd, J = 1.0, 7.0, 8.1 Hz, 1H), 5.05 (quin, J = 6.2 Hz, 1H), 4.16 (t, J = 5.9 Hz, 2H), 3.97 (br s, 2H), 3.67 (t, J = 6.5 Hz, 2H), 2.26 (quin, J = 6.3 Hz, 2H), 1.51 (s, 6H), 1.18 (d, J = 6.2 Hz, 6H). MS (ES, [M + H]$^+$), m/z 538.9.

Isopropyl 3-[4-(2-Bromoethoxy)benzoyl]-1,1-dimethyl-1,2,3,6-tetrahydroazepino[4,5-*b*]indole-5-carboxylate 13j−n. ^{1}H NMR (400 MHz, DMSO-d_6) δ 10.83 (s, 1H), 7.76 (d, J = 8.2 Hz, 1H), 7.74 (s, 1H), 7.57−7.50 (m, 3H), 7.09−7.06 (m, 3H), 6.98 (ddd, J = 1.1, 7.0, 8.1 Hz, 1H), 5.05 (quin, J = 6.2 Hz, 1H), 4.40 (t, J = 5.3 Hz, 2H), 3.97 (br s, 2H), 3.83 (t, J = 5.3 Hz, 2H), 1.51 (s, 6H), 1.18 (d, 6H). MS (ES, [M + H]$^+$), m/z 524.9.

Isopropyl 3-[3-(2-Bromoethoxy)benzoyl]-1,1-dimethyl-1,2,3,6-tetrahydroazepino[4,5-*b*]indole-5-carboxylate 13s−w. ^{1}H NMR (400 MHz, DMSO-d_6) δ 10.82 (s, 1H), 7.76 (d, J = 8.0 Hz, 1H), 7.70 (s, 1H), 7.54 (d, J = 8.0 Hz, 1H), 7.44 (t, J = 8.2 Hz, 1H), 7.21 (ddd, J = 1.1, 2.5, 8.4 Hz, 1H), 7.13−7.05 (m, 3H), 6.98 (ddd, J = 1.1, 7.0, 8.1 Hz, 1H), 5.03 (quin, J = 6.2 Hz, 1H), 4.36 (t, J = 5.3 Hz, 2H), 3.97 (br s, 2H), 3.80 (t, J = 5.3 Hz, 2H), 1.52 (s, 6H), 1.16 (d, J = 6.2 Hz, 6H); HRMS: calcd for $C_{27}H_{29}BrN_2O_4$ + H$^+$, 525.1383; found (ESI, [M + H]$^+$), 525.1380.

Isopropyl 3-[3-(3-Bromopropoxy)benzoyl]-1,1-dimethyl-1,2,3,6-tetrahydroazepino[4,5-*b*]indole-5-carboxylate 13x−bb. ^{1}H NMR (400 MHz, DMSO-d_6) δ 10.82 (s, 1H), 7.76 (d, J = 8.2 Hz, 1H), 7.70 (s, 1H), 7.54 (ddd, J = 1.0, 1.0, 8.0 Hz, 1H), 7.43 (t, J = 7.94 Hz, 1H), 7.20 (ddd, J = 1.0, 2.5, 8.3 Hz, 1H), 7.12−7.04 (m, 3H), 6.98 (ddd, J = 1.0, 7.0, 8.1 Hz, 1H), 5.03 (quin, J = 6.2 Hz, 1H), 4.12 (t, J = 6.0 Hz, 2H), 3.97 (br s, 2H), 3.65 (t, J = 6.5 Hz, 2H), 2.24 (quin, J = 6.3 Hz, 2H), 1.52 (s, 6H), 1.16 (d, J = 6.2 Hz, 6H); MS (ES, [M + H]$^+$), m/z 538.8.

General Procedure for the Synthesis of Oxygen-tethered Amines 14i−bb. To a solution of alkyl bromide (**13i−bb**) (50 μmol) in 1-methyl-2-pyrrolidinone (0.5 mL) was added the appropriate amine (300 μmol). The reaction was stirred at room temperature for 18 h. The reaction was concentrated under reduced pressure and the crude mixture was added to a Gilson sample tube containing TEA (50 μL) and methanol (200 μL). The reaction vessel was rinsed into the sample tube with methanol (400 μL followed by 200 μL). Distilled water (200 μL) was added to the sample tube and the crude was purified by RP-HPLC using a Gilson automated HPLC system and collector: Column; Sunfire prep C18, 5 μ, 19 × 50 mm. Isocratic 10/90 acetonitrile/Water (10 mL/min, no modifier) for 1.6 min followed by a gradient to 100% acetonitrile (20 mL/min, no modifier) at 9.5 min; then hold for three min at 100% acetonitrile and ramp back to 10% acetonitrile in water over 2.0 min. Desired fractions were combined and lyophilized to give the titled products (**14i−bb**) (16−70% yields).

Isopropyl 1,1-Dimethyl-3-[4-(3-morpholin-4-ylpropoxy)benzoyl]-1,2,3,6-tetrahydroazepino[4,5-*b*]indole-5-carboxylate 14i. ^{1}H NMR (400 MHz, DMSO-d_6) δ 10.83 (s, 1H), 7.74 (s, 1H), 7.76−7.73 (m, 1H), 7.55 (ddd, J = 1.0, 1.0, 8.0 Hz, 1H), 7.51 (d, J = 9.0 Hz, 2H), 7.10−7.06 (m, 1H), 7.04 (d, J = 9.0 Hz, 2H), 6.97 (ddd, J = 1.0, 7.0, 8.1 Hz, 1H), 5.05 (quin, J = 6.2 Hz, 1H), 4.09 (t, J = 6.3 Hz, 2H), 3.97 (br s, 2H), 3.56 (t, J = 4.5 Hz, 4H), 2.41 (t, J = 7.1 Hz, 2H), 2.38−2.31 (m, 4H), 1.88 (quin, J = 6.7 Hz, 2H), 1.51 (s, 6H), 1.18 (d, J = 6.2 Hz, 6H); HRMS: calcd for $C_{32}H_{39}N_3O_5$ + H$^+$, 546.2962; found (ESI, [M + H]$^+$), 546.2962; Analytical HPLC: R_t = 10.2 min (100%).

Isopropyl 1,1-Dimethyl-3-[4-(2-piperidin-1-ylethoxy)benzoyl]-1,2,3,6-tetrahydroazepino[4,5-*b*]indole-5-carboxylate 14j. ^{1}H NMR (400 MHz, DMSO-d_6) δ 10.84 (s, 1H), 7.78−7.73 (m, 2H), 7.55 (d, J = 7.8 Hz, 1H), 7.51 (d, J = 9.0 Hz, 2H), 7.10−7.04 (m, 3H), 6.98 (ddd, J = 1.0, 7.0, 8.1 Hz, 1H), 5.05 (quin, J = 6.2 Hz, 1H), 4.14 (t, J = 5.9 Hz, 2H), 3.97 (br s, 2H), 2.65 (t, J = 5.9 Hz, 2H), 2.45−2.37 (m, 4H), 1.51 (s, 6H), 1.45−1.51 (m, 6H), 1.18 (d, J = 6.2 Hz, 6H); HRMS: calcd for $C_{32}H_{39}N_3O_4$ + H$^+$, 530.3013; found (ESI, [M+H]$^+$), 530.3015; Analytical HPLC: R_t = 10.2 min (99.5%).

Isopropyl 3-{4-[2-(Dimethylamino)ethoxy]benzoyl}-1,1-dimethyl-1,2,3,6-tetrahydroazepino[4,5-*b*]indole-5-carboxylate 14k. ^{1}H NMR (400 MHz, CDCl$_3$) δ 10.72 (s, 1H), 7.89 (s, 1H), 7.82 (dd, J = 1.0, 8.0 Hz, 1H), 7.58 (d, J = 8.9 Hz, 2H), 7.38 (d, J = 8.0 Hz, 1H), 7.17 (ddd, J = 1.0, 7.0, 8.1 Hz, 1H), 7.07 (ddd, J = 1.0, 7.0, 8.1 Hz, 1H), 6.94 (d, J = 8.9 Hz, 2H), 5.14 (quin, J = 6.2 Hz, 1H), 4.11 (t, J = 5.6 Hz, 2H), 4.08 (br s, 2H), 2.75 (t, J = 5.5 Hz, 2H), 2.34 (s, 6H), 1.62 (s, 6H), 1.21 (d, J = 6.2 Hz, 6H); HRMS: calcd for $C_{29}H_{35}N_3O_4$ + H$^+$, 490.2700; found (ESI, [M + H]$^+$), 490.2701; Analytical HPLC: R_t = 9.9 min. (97.1%).

Isopropyl 1,1-Dimethyl-3-[4-(2-pyrrolidin-1-ylethoxy)benzoyl]-1,2,3,6-tetrahydroazepino[4,5-*b*]indole-5-carboxylate 14l. ^{1}H NMR (400 MHz, CDCl$_3$) δ 10.72 (s, 1H), 7.89 (s, 1H), 7.81 (dd, J = 1.0, 8.0 Hz, 2H), 7.58 (d, J = 8.78 Hz, 2H), 7.38 (ddd, J = 1.0, 1.0, 8.0 Hz, 1H), 7.17 (ddd, J = 1.0, 7.0, 8.0 Hz, 1H), 7.07 (ddd, J = 1.0, 7.0, 8.0 Hz, 1H), 6.93 (d, J = 9.0 Hz, 2H), 5.14 (quin, J = 6.2 Hz, 1H), 4.15 (t, J = 5.90 Hz, 2H), 4.09 (br s, 2H), 2.92 (t, J = 5.9 Hz, 2H), 2.66−2.59 (m, 4H), 1.83−1.80 (m, 4H), 1.62 (s, 6H), 1.21 (d, J = 6.2 Hz, 6H); HRMS: calcd for $C_{31}H_{37}N_3O_4$ + H$^+$, 516.2857; found (ESI, [M + H]$^+$), 516.2859; Analytical HPLC: R_t = 10.1 min. (95.5%).

Isopropyl 1,1-Dimethyl-3-[4-(2-morpholin-4-ylethoxy)benzoyl]-1,2,3,6-tetrahydroazepino[4,5-*b*]indole-5-carboxylate 14m. ^{1}H NMR (400 MHz, DMSO-d_6) δ 10.83 (s, 1H), 7.77−7.74 (m, 2H), 7.55 (ddd, J = 1.0, 1.0, 8.0 Hz, 1H), 7.51 (d, J = 9.0 Hz, 2H), 7.10−7.04 (m, 3H), 6.98 (ddd, J = 1.0, 7.0, 8.0 Hz, 1H), 5.05 (quin, J = 6.2 Hz, 1H), 4.16 (t, J = 5.7 Hz, 2H), 3.97 (br s, 2H), 3.57 (t, J = 4.6 Hz, 4H), 2.70 (t, J = 5.6 Hz, 2H), 2.48−2.43 (m, 4H), 1.51 (s, 6H), 1.18 (d, J = 6.2 Hz, 6H); HRMS: calcd for $C_{31}H_{37}N_3O_5$ + H$^+$, 532.2806; found (ESI, [M + H]$^+$), 532.2811; Analytical HPLC: R_t = 10.6 min (98.9%).

Isopropyl 1,1-Dimethyl-3-{4-[2-(4-methylpiperazin-1-yl)ethoxy]-benzoyl}-1,2,3,6-tetrahydroazepino[4,5-*b*]indole-5-carboxylate 14n. ^{1}H NMR (400 MHz, CDCl$_3$) δ 10.71 (s, 1H), 7.89 (s, 1H), 7.82 (dd, J = 1.0, 8.0 Hz, 1H), 7.58 (d, J = 8.9 Hz, 2H), 7.38 (ddd, J = 1.0, 1.0, 8.0 Hz, 1H), 7.17 (ddd, J = 1.0, 7.0, 8.0 Hz, 1H), 7.07 (ddd, J = 1.0, 7.0, 8.0 Hz, 1H), 6.92 (d, J = 8.9 Hz, 2H), 5.14 (quin, J = 6.2 Hz, 1H), 4.15 (t, J = 5.8 Hz, 2H), 4.12 (br s, 2H), 2.83 (t, J = 5.8 Hz, 2H), 2.63 (br s, 4H), 2.48 (br s, 4H), 2.30 (s, 3H), 1.62 (s, 6H), 1.22 (d, J = 6.2 Hz, 6H); HRMS: calcd for $C_{32}H_{40}N_4O_4$ + H$^+$, 545.3122; found (ESI, [M + H]$^+$), 545.3125; Analytical HPLC: R_t = 10.2 min (98.5%).

Isopropyl 3-{4-[3-(Dimethylamino)propoxy]benzoyl}-1,1-di-methyl-1,2,3,6-tetrahydroazepino[4,5-*b*]indole-5-carboxylate 14o. ^{1}H NMR (400 MHz, CDCl$_3$) δ 10.72 (s, 1H), 7.89 (s, 1H), 7.82 (dd, J = 1.0, 8.0 Hz, 1H), 7.57 (d, J = 9.0 Hz, 2H), 7.38 (ddd, J = 1.0, 1.0, 8.0 Hz, 1H), 7.17 (ddd, J = 1.0, 7.0, 8.0 Hz, 1H), 7.07 (ddd, J = 1.0, 7.0, 8.0 Hz, 1H), 6.91 (d, J = 8.8 Hz, 2H), 5.14 (quin, J = 6.2 Hz, 1H), 4.06 (t, J = 6.4 Hz, 2H), 4.01 (br s, 2H), 2.45 (t, J = 7.2 Hz, 2H), 2.25 (s, 6H), 1.97 (quin, J = 6.8 Hz, 2H), 1.62 (s, 6H), 1.22 (d, J = 6.2 Hz, 6H); HRMS: calcd for $C_{30}H_{37}N_3O_4$ + H$^+$, 504.2857; found (ESI, [M + H]$^+$), 504.2857; Analytical HPLC: R_t = 10.1 min (82.5%).

Isopropyl 1,1-Dimethyl-3-[4-(3-pyrrolidin-1-ylpropoxy)benzoyl]-1,2,3,6-tetrahydroazepino[4,5-*b*]indole-5-carboxylate 14p. ^{1}H NMR (400 MHz, CDCl$_3$) δ 10.72 (s, 1H), 7.89 (s, 1H), 7.82 (dd, J = 1.0, 8.0 Hz, 1H), 7.57 (d, J = 8.8 Hz, 2H), 7.38 (ddd, J = 1.0, 1.0, 8.0 Hz, 1H), 7.17 (ddd, J = 1.0, 7.0, 8.0 Hz, 1H), 7.07 (ddd, 1H), 6.91 (d, J = 9.0 Hz, 2H), 5.14 (quin, J = 6.2 Hz, 1H), 4.08 (t, J = 6.4 Hz, 2H), 4.03 (br s, 2H), 2.64 (t, J = 7.4 Hz, 2H), 2.59−2.49 (m, 4H), 2.06−2.00 (m, 2H), 1.82−1.78 (m, 4H), 1.62 (s, 6H), 1.22 (d, J = 6.2 Hz, 6H); HRMS: calcd for $C_{32}H_{39}N_3O_4$ + H$^+$, 530.3013; found (ESI, [M + H]$^+$), 530.3016; Analytical HPLC: R_t = 10.3 min (75.2%).

Isopropyl 1,1-Dimethyl-3-[4-(3-piperidin-1-ylpropoxy)benzoyl]-1,2,3,6-tetrahydroazepino[4,5-*b*]indole-5-carboxylate 14q. ^{1}H NMR (400 MHz, CDCl$_3$) δ 10.71 (s, 1H), 7.89 (s, 1H), 7.82 (dd, J = 1.0, 8.0 Hz, 1H), 7.58 (d, J = 8.8 Hz, 2H), 7.39 (ddd, J = 1.0, 1.0, 8.0 Hz, 1H), 7.17 (ddd, J = 1.0, 7.0, 8.0 Hz, 1H), 7.07 (ddd, J = 1.0, 7.0, 8.0 Hz, 1H), 6.90 (d, J = 8.8 Hz, 2H), 5.15 (quin, J = 6.2 Hz, 1H), 4.07 (t, J = 6.2 Hz, 2H), 4.00 (br s, 2H), 2.71−2.55 (m, 6H), 2.16−2.06 (m, 2H), 1.76−1.66 (m, 4H), 1.62 (s, 6H), 1.50 (br s, 2H), 1.22 (d, J = 6.2 Hz, 6H); HRMS: calcd for $C_{33}H_{41}N_3O_4$ + H$^+$, 544.3170; found (ESI, [M + H]$^+$), 544.3172; Analytical HPLC: R_t = 10.4 min (100%).

Isopropyl 1,1-Dimethyl-3-{4-[3-(4-methylpiperazin-1-yl)pro-poxy]benzoyl}-1,2,3,6-tetrahydroazepino[4,5-*b*]indole-5-carboxy-late 14r. ^{1}H NMR (400 MHz, CDCl$_3$) δ 10.71 (s, 1H), 7.89 (s, 1H), 7.82 (dd, J = 1.0, 8.0 Hz, 1H), 7.58 (d, J = 8.8 Hz, 2H), 7.38 (ddd, J = 1.0, 1.0, 8.0 Hz, 1H), 7.17 (ddd, J = 1.0, 7.0, 8.0 Hz, 1H), 7.07 (ddd, J = 1.0, 7.0, 8.0 Hz, 1H), 6.91 (d, J = 8.8 Hz, 2H), 5.14 (quin, J = 6.2 Hz, 1H), 4.06 (t, J = 6.4 Hz, 2H), 4.00 (br s, 2H), 2.57−2.49 (m, 2H), 2.45 (br s, 8H), 2.29 (s, 3H), 1.94−2.03 (m, 2H), 1.62 (s, 6H), 1.22 (d, J = 6.2 Hz, 6H); HRMS: calcd for $C_{33}H_{42}N_4O_4$ + H$^+$, 559.3279; found (ESI, [M + H]$^+$), 559.3280; Analytical HPLC: R_t = 10.4 min (91.4%).

Isopropyl 3-{3-[2-(Dimethylamino)ethoxy]benzoyl}-1,1-dimethyl-1,2,3,6-tetrahydroazepino[4,5-*b*]indole-5-carboxylate 14s. ^{1}H NMR (400 MHz, CDCl$_3$) δ 10.71 (s, 1H), 7.84 (s, 1H), 7.82 (d, J = 8.0 Hz, 1H), 7.38 (ddd, J = 1.0, 1.0, 8.0 Hz, 1H), 7.31 (t, J = 8.0 Hz, 1H), 7.20−7.14 (m, 2H), 7.12−7.04 (m, 3H), 5.12 (quin, J = 6.2 Hz, 1H), 4.10 (t, J = 5.6 Hz, 2H), 4.02 (br s, 2H), 2.76 (t, J = 5.6 Hz, 2H), 2.35 (s, 6H), 1.63 (s, 6H), 1.19 (d, J = 6.2 Hz, 6H); HRMS: calcd for $C_{29}H_{35}N_3O_4$ + H$^+$, 490.2700; found (ESI, [M + H]$^+$), 490.2691; Analytical HPLC: R_t = 9.8 min (98.8%).

Isopropyl 1,1-Dimethyl-3-[3-(2-pyrrolidin-1-ylethoxy)benzoyl]-1,2,3,6-tetrahydroazepino[4,5-*b*]indole-5-carboxylate 14t. ^{1}H NMR (400 MHz, CDCl$_3$) δ 10.71 (s, 1H), 7.84 (s, 1H), 7.82 (dd, J = 1.0, 8.0 Hz, 1H), 7.38 (ddd, J = 1.0, 1.0, 8.2 Hz, 1H), 7.31 (t, J = 7.9 Hz, 1H), 7.20−7.14 (m, 2H), 7.11−7.05 (m, 3H), 5.12 (quin, J = 6.2 Hz, 1H), 4.16 (t, J = 5.6 Hz, 2H), 4.09 (br s, 2H), 2.96 (t, J = 5.6 Hz, 2H), 2.69 (br s, 4H), 1.88−1.79 (m, 4H), 1.63 (s, 6H), 1.19 (d, J = 6.2 Hz, 6H); HRMS: calcd for $C_{31}H_{37}N_3O_4$ + H$^+$, 516.2857; found (ESI, [M + H]$^+$), 516.2850; Analytical HPLC: R_t = 10.0 min (83.3%).

Isopropyl 1,1-Dimethyl-3-[3-(2-piperidin-1-ylethoxy)benzoyl]-1,2,3,6-tetrahydroazepino[4,5-*b*]indole-5-carboxylate 14u. ^{1}H NMR (400 MHz, CDCl$_3$) δ 10.71 (s, 1H), 7.84 (s, 1H), 7.82 (dd, J = 1.0, 8.0 Hz, 1H), 7.38 (ddd, J = 1.0, 1.0, 8.0 Hz, 1H), 7.31 (t, J = 8.0 Hz, 1H), 7.17 (ddd, J = 1.0, 7.0, 8.0 Hz, 1H), 7.14 (dd, J = 1.4, 2.5 Hz, 1H), 7.11−7.04 (m, 3H), 5.12 (quin, J = 6.2 Hz, 1H), 4.13 (t, J = 5.9 Hz, 2H), 4.08 (br s, 2H), 2.79 (t, J = 5.9 Hz, 2H), 2.52 (br s, 4H), 1.63 (s, 6H), 1.62−1.56 (m, 4H), 1.48−1.40 (m, 2H), 1.19 (d, J = 6.2 Hz, 6H); HRMS: calcd for $C_{32}H_{39}N_3O_4$ + H$^+$, 530.3013; found (ESI, [M + H]$^+$), 530.3006; Analytical HPLC: R_t = 10.1 min (95.6%).

Isopropyl 1,1-Dimethyl-3-[3-(2-morpholin-4-ylethoxy)benzoyl]-1,2,3,6-tetrahydroazepino[4,5-*b*]indole-5-carboxylate 14v. ^{1}H NMR (400 MHz, CDCl$_3$) δ 10.70 (s, 1H), 7.85−7.80 (m, 2H), 7.38 (ddd, J = 1.0, 1.0, 8.0 Hz, 1H), 7.32 (t, J = 8.0 Hz, 1H), 7.21−7.13 (m, 2H), 7.13−7.03 (m, 3H), 5.12 (quin, J = 6.2 Hz, 1H), 4.13 (t, J = 5.4 Hz, 2H), 4.04 (br s, 2H), 3.72 (t, J = 4.3 Hz, 4H), 2.81 (t, J = 4.3 Hz, 2H), 2.57 (br s, 4H), 1.63 (s, 6H), 1.19 (d, J = 6.2 Hz, 6H); HRMS: calcd for $C_{31}H_{37}N_3O_5$ + H$^+$, 532.2806; found (ESI, [M + H]$^+$), 532.2799; Analytical HPLC: R_t = 10.5 min (100%).

Isopropyl 1,1-Dimethyl-3-{3-[2-(4-methylpiperazin-1-yl)ethoxy]-benzoyl}-1,2,3,6-tetrahydroazepino[4,5-*b*]indole-5-carboxylate 14w. ^{1}H NMR (400 MHz, CDCl$_3$) δ 10.70 (s, 1H), 7.84 (s, 1H), 7.82 (d, J = 8.2 Hz, 1H), 7.38 (dd, J = 1.0, 8.2 Hz, 1H), 7.31 (t, J = 7.9 Hz, 1H), 7.21−7.13 (m, 2H), 7.13−7.04 (m, 3H), 5.12 (quin, J = 6.2 Hz, 1H), 4.11 (t, J = 5.6 Hz, 2H), 4.03 (br s, 2H), 2.82 (t, J = 5.6 Hz, 2H), 2.65 (br s, 4H), 2.52 (br s, 4H), 2.32 (s, 3H), 1.63 (s, 6H), 1.19 (d, J = 6.2 Hz, 6H); HRMS: calcd for $C_{32}H_{40}N_4O_4$ + H$^+$, 545.3122; found (ESI, [M + H]$^+$), 545.3116; Analytical HPLC: R_t = 10.1 min (97.3%).

Isopropyl 3-{3-[3-(Dimethylamino)propoxy]benzoyl}-1,1-di-methyl-1,2,3,6-tetrahydroazepino[4,5-*b*]indole-5-carboxylate 14x. ^{1}H NMR (400 MHz, CDCl$_3$) δ 10.71 (s, 1H), 7.85 (s, 1H), 7.82 (d, J = 8.2 Hz, 1H), 7.38 (ddd, J = 1.0, 1.0, 8.0 Hz, 1H), 7.31 (t, J = 8.0 Hz, 1H), 7.17 (ddd, J = 1.0, 7.0, 8.0 Hz, 1H), 7.14 (dd, J = 1.6, 2.5 Hz, 1H), 7.10−7.07 (m, 2H), 7.07−7.03 (m, 1H), 5.12 (quin, J = 6.2 Hz, 1H), 4.08 (br s, 2H), 4.03 (t, J = 6.4 Hz, 2H), 2.48 (t, J = 7.3 Hz, 2H), 2.27 (s, 6H), 1.98 (dd, J = 6.4, 7.3 Hz, 2H), 1.63 (s, 6H), 1.19 (d, J = 6.2 Hz, 6H); HRMS: calcd for $C_{30}H_{37}N_3O_4$ + H$^+$, 504.2857; found (ESI, [M + H]$^+$), 504.2850; Analytical HPLC: R_t = 10.0 min (98.5%).

Isopropyl 1,1-Dimethyl-3-[3-(3-pyrrolidin-1-ylpropoxy)benzoyl]-1,2,3,6-tetrahydroazepino[4,5-*b*]indole-5-carboxylate 14y. ^{1}H NMR (400 MHz, CDCl$_3$) δ 10.71 (s, 1H), 7.85 (s, 1H), 7.82 (dd, J = 1.0, 8.0 Hz, 1H), 7.38 (ddd, J = 1.0, 1.0, 8.0 Hz, 1H), 7.31 (t, J = 7.8 Hz, 1H), 7.17 (ddd, J = 1.0, 8.0, 8.0 Hz, 1H), 7.15−7.11 (m, 1H), 7.11−7.03 (m, 3H), 5.12 (quin, J = 6.2 Hz, 1H), 4.10 (br s, 2H), 4.05 (t, J = 6.3 Hz, 2H), 2.67−2.76 (m, 2H), 2.63 (br s, 4H), 2.12−2.02 (m, 2H), 1.89−1.80 (m, 4H), 1.63 (s, 6H), 1.19 (d, J = 6.2 Hz, 6H); HRMS: calcd for $C_{32}H_{39}N_3O_4$ + H$^+$, 530.3013; found (ESI, [M + H]$^+$), 530.3006; Analytical HPLC: R_t = 10.2 min (88.3%).

Isopropyl 1,1-Dimethyl-3-[3-(3-piperidin-1-ylpropoxy)benzoyl]-1,2,3,6-tetrahydroazepino[4,5-*b*]indole-5-carboxylate 14z. ^{1}H NMR (400 MHz, CDCl$_3$) δ 10.71 (s, 1H), 7.86 (s, 1H), 7.82 (dd, J = 1.0,

8.0 Hz, 1H), 7.38 (ddd, J = 1.0, 1.0, 8.0 Hz, 1H), 7.30 (t, J = 8.0 Hz, 1H), 7.17 (ddd, J = 1.0, 7.0, 8.0 Hz, 1H), 7.13 (dd, J = 1.5, 2.5 Hz, 1H), 7.10−7.07 (m, 2H), 7.07−7.03 (m, 1H), 5.12 (quin, J = 6.2 Hz, 1H), 4.07 (br s, 2H), 4.02 (t, J = 6.3 Hz, 2H), 2.49 (t, J = 7.4 Hz, 2H), 2.42 (br s, 4H), 2.03−1.95 (m, 2H), 1.63 (s, 6H), 1.62−1.56 (m, 4H), 1.48−1.40 (m, 2H), 1.19 (d, J = 6.2 Hz, 6H); HRMS: calcd for $C_{33}H_{41}N_3O_4$ + H^+, 544.3170; found (ESI, $[M + H]^+$), 544.3162; Analytical HPLC: R_t = 10.3 min (90.0%).

Isopropyl 1,1-Dimethyl-3-[3-(3-morpholin-4-ylpropoxy)benzoyl]-1,2,3,6-tetrahydroazepino[4,5-*b*]indole-5-carboxylate 14aa. ^{1}H NMR (400 MHz, CDCl$_3$) δ 10.70 (s, 1H), 7.85 (s, 1H), 7.82 (dd, J = 1.0, 8.0 Hz, 1H), 7.38 (ddd, J = 1.0, 1.0, 8.0 Hz, 1H), 7.31 (t, J = 8.0 Hz, 1H), 7.18 (ddd, J = 1.0, 7.0, 8.0 Hz, 1H), 7.14 (dd, J = 1.5, 2.5 Hz, 1H), 7.11−7.03 (m, 3H), 5.12 (quin, J = 6.2 Hz, 1H), 4.08 (br s, 2H), 4.03 (t, J = 4.6 Hz, 4H), 2.51 (t, J = 7.2 Hz, 2H), 2.48−2.42 (m, 4H), 2.01−1.93 (m, 2H), 1.63 (s, 6H), 1.19 (d, J = 6.2 Hz, 6H); HRMS: calcd for $C_{32}H_{39}N_3O_5$ + H^+, 546.2963; found (ESI, $[M + H]^+$), 546.2959; Analytical HPLC: R_t = 10.3 min (99.6%).

Isopropyl 1,1-Dimethyl-3-{3-[3-(4-methylpiperazin-1-yl)propoxy]benzoyl}-1,2,3,6-tetrahydroazepino[4,5-*b*]indole-5-carboxylate 14bb. ^{1}H NMR (400 MHz, CDCl$_3$) δ 10.71 (s, 1H), 7.86 (s, 1H), 7.82 (d, J = 8.0 Hz, 1H), 7.38 (dd, J = 1.0, 8.0 Hz, 1H), 7.34−7.27 (m, 1H), 7.21−7.15 (m, 1H), 7.14−7.02 (m, 4H), 5.12 (quin, J = 6.2 Hz, 1H), 4.06 (br s, 2H), 4.02 (t, J = 6.2 Hz, 2H), 2.59−2.44 (m, 6H), 2.31 (s, 3H), 2.01−1.94 (m, 2H), 1.63 (s, 6H), 1.58 (br s, 4H), 1.19 (d, J = 6.2 Hz, 6H); HRMS: calcd for $C_{33}H_{42}N_4O_4$ + H^+, 559.3279; found (ESI, $[M + H]^+$), 559.3271; Analytical HPLC: R_t = 10.3 min (98.5%).

General Procedure for the Synthesis of Linker 15cc−dd. To a solution of benzyl-4-hydroxybenzoate (100 mg, 0.438 mmol) and either bromoethanol or bromopropanol (0.797 mmol) in THF (2 mL) was added either DIAD or DEAD (0.789 mmol) followed by triphenylphosphine (208 mg, 0.797 mmol) in portions at room temperature with stirring. After 1 h, the reaction was concentrated to near dryness, diluted with diethyl ether, and washed with water. The organic layer was dried over magnesium sulfate, filtered, concentrated to a small volume, and placed in a freezer. After 2 h, triphenylphosphine oxide precipitated out of solution. The solution was decanted, concentrated, and purified by flash column chromatography (EtOAc/hexane 0:100−20:80) to yield the desired product (**15cc−dd**) (78−82% yields).

Benzyl 4-(3-Bromopropoxy)benzoate 15cc. ^{1}H NMR (400 MHz, DMSO-d_6) δ 7.95 (d, J = 9.0 Hz, 2H), 7.49−7.31 (m, 5H), 7.07 (d, J = 9.0 Hz, 2H), 5.32 (s, 2H), 4.16 (t, J = 6.0 Hz, 2H), 3.67 (t, J = 6.5 Hz, 2H), 2.27 (quin, J = 6.3 Hz, 2H); MS (ES, $[M + H]^+$), m/z 348.9, 350.9.

Benzyl 4-(2-Bromoethoxy)benzoate 15dd. ^{1}H NMR (400 MHz, DMSO-d_6) δ 7.95 (d, J = 9.0 Hz, 2H), 7.49−7.32 (m, 5H), 7.08 (d, J = 9.0 Hz, 2H), 5.32 (s, 2H), 4.41 (t, J = 5.4 Hz, 2H), 3.83 (t, J = 5.4 Hz, 2H); MS (ES, $[M + H]^+$), m/z 334.9, 336.9.

General Procedure for the Synthesis of Protected Amine Linker 16cc−dd. To a solution of alkyl bromide (**15cc−dd**) (28.7 mmol) in acetonitrile (100 mL) was added morpholine (15 mL, 172 mmol). The reaction was stirred at room temperature for 18 h, at which time the reaction was concentrated to near dryness, diluted with EtOAc, and washed with water. The aqueous layer was extracted with EtOAc and the combined organic layers were washed with saturated sodium bicarbonate, water, and brine. The organic layer was dried over magnesium sulfate, filtered, and concentrated to yield the desired product (**16cc−dd**) (97−100% yields).

Benzyl 4-(3-Morpholin-4-ylpropoxy)benzoate 16cc. ^{1}H NMR (400 MHz, DMSO-d_6) δ 7.94 (d, J = 9.0 Hz, 2H), 7.48−7.31 (m, 5H), 7.04 (d, J = 9.0 Hz, 2H), 5.31 (s, 2H), 4.09 (t, J = 6.4 Hz, 2H), 3.59−3.53 (m, 4H), 2.41 (t, J = 7.2 Hz, 2H), 2.38−2.32 (m, 4H), 1.89 (quin, J = 6.8 Hz, 2H); MS (ES, $[M + H]^+$), m/z 356.3.

Benzyl 4-(2-Morpholin-4-ylethoxy)benzoate 16dd. ^{1}H NMR (400 MHz, DMSO-d_6) δ 7.93 (d, J = 8.8 Hz, 2H), 7.48−7.32 (m, 5H), 7.06 (d, J = 8.8 Hz, 2H), 5.31 (s, 2H), 4.17 (t, J = 5.7 Hz, 2H), 3.60−3.54 (m, 4H), 2.70 (t, J = 5.7 Hz, 2H), 2.49−2.43 (m, 4H); HRMS: calcd for $C_{20}H_{23}NO_4$ + H^+, 342.1700; found (ESI, $[M + H]^+$), 342.1705.

General Procedure for the Deprotection of Ester 17cc−dd. To a solution of the benzyl ester (**16cc−dd**) (2.25 mmol) in methanol (54 mL) and EtOAc (6 mL) was added cyclohexadiene (2.14 mL, 22.6 mmol) and 20% palladium hydroxide on carbon (570 mg). The reaction was flushed with nitrogen and capped with a rubber septum. To relieve pressure build-up, the septum was pierced with a needle attached to an empty balloon. The sealed system was heated at 64 °C for 1 h. Upon completion, the reaction was filtered through Celite, washed with methanol and concentrated to dryness and further dried under vacuum for 2 h. The desired product (**17cc−dd**) was used in the next reaction without further purification (94−95% yields).

4-(3-Morpholin-4-ylpropoxy)benzoic Acid 17cc. ^{1}H NMR (400 MHz, DMSO-d_6) δ 11.91 (br s, 1H), 7.88 (d, J = 9.0 Hz, 2H), 6.99 (d, J = 9.0 Hz, 2H), 4.07 (t, J = 6.4 Hz, 2H), 3.60−3.53 (m, 4H), 2.41 (t, J = 7.2 Hz, 2H), 2.38−2.31 (m, 4H), 1.94−1.84 (m, 2H); MS (ES, $[M + H]^+$), m/z 265.9.

4-(2-Morpholin-4-ylethoxy)benzoic Acid 17dd. ^{1}H NMR (400 MHz, DMSO-d_6) δ 12.56 (br s, 1H), 7.88 (d, J = 8.8 Hz, 2H), 7.03 (d, J = 8.8 Hz, 2H), 4.17 (t, J = 5.7 Hz, 2H), 3.63−3.54 (m, 4H), 2.73 (br s, 2H), 2.48 (br s, 4H); HRMS: calcd for $C_{13}H_{17}NO_4$ + H^+, 252.1230; found (ESI, $[M + H]^+$), 252.1238.

General Procedure for the Formation of Benzoyl Chlorides. A solution of the appropriate benzoic acid **17cc** or **17dd** (2.25 mmol) and thionyl chloride (62 mmol, 4.5 mL) was heated at 78 °C for 2−4 h. The reaction was then concentrated to dryness. Toluene was added and the resulting solution was concentrated. The toluene concentration procedure was repeated (× 2). The crude material was dried on a vacuum pump for 1−2 h to provide the desired product which was used in the next reaction without further purification.

General Procedure for the Acylation of Indoleazepines 14cc−dd. To a solution of the appropriate benzoyl chloride (previous step, 2.25 mmol) suspended in acetonitrile (16 mL) was added a solution of isopropyl 8-fluoro-1,1-dimethyl-l,2,3,6-tetrahydroazepino[4,5-*b*]indole-5-carboxylate (**9**) (474 mg, 1.5 mmol) and TEA (627 μL, 4.5 mmol) in acetonitrile (4 mL). The reaction was stirred overnight at which time methanol (2 mL) was added and the reaction was concentrated. The crude material was partitioned between EtOAc (50 mL) and saturated sodium bicarbonate (50 mL). The organic layer was separated and the aqueous layer was extracted again with EtOAc. The organic layers were combined and washed with brine and water and dried over magnesium sulfate. The resulting crude product was purified via flash column chromatography two times (methanol/CH$_2$Cl$_2$ 0:100−10:90). The desired product (**14cc** or **14dd**) was obtained by crystallization of the purified material from acetonitrile (78−87% yields).

Isopropyl 8-Fluoro-1,1-dimethyl-3-[4-(3-morpholin-4-ylpropoxy)benzoyl]-1,2,3,6-tetrahydroazepino[4,5-*b*]indole-5-carboxylate 14cc. ^{1}H NMR (400 MHz, DMSO-d_6) δ 10.97 (s, 1H), 7.79−7.72 (m, 2H), 7.55 (d, J = 8.8 Hz, 2H), 7.36 (dd, J = 2.5, 10.2 Hz, 1H), 7.06 (d, J = 8.8 Hz, 2H), 6.83 (ddd, J = 2.5, 9.3, 9.3 Hz, 1H), 5.05 (quin, J = 6.2 Hz, 1H), 4.14 (t, J = 5.9 Hz, 2H), 3.99 (br s, 2H), 3.96 (br s, 2H), 3.75 (ddd, J = 1.0, 12.3, 12.3 Hz, 2H), 3.46 (d, J = 12.3 Hz, 2H), 3.31−3.23 (m, 2H), 3.15−3.02 (m, 2H), 2.24−2.14 (m, 2H), 1.49 (s, 6H), 1.18 (d, J = 6.2 Hz, 6H); HRMS: calcd for $C_{32}H_{38}FN_3O_5$ + H^+, 564.2868; found (ESI, $[M + H]^+$), 564.2869; Analytical HPLC: R_t = 10.7 min (100%).

Isopropyl 8-Fluoro-1,1-dimethyl-3-[4-(2-morpholin-4-ylethoxy)benzoyl]-1,2,3,6-tetrahydroazepino[4,5-*b*]indole-5-carboxylate 14dd. ^{1}H NMR (400 MHz, DMSO-d_6) δ 10.97 (s, 1H), 7.78−7.74 (m, 1H), 7.74 (s, 1H), 7.57 (d, J = 9.0 Hz, 2H), 7.36 (dd, J = 2.5, 10.2 Hz, 1H), 7.13 (d, J = 9.0 Hz, 2H), 6.87−6.80 (m, 1H), 5.05 (quin, J = 6.2 Hz, 1H), 4.51−4.45 (m, 2H), 4.01−3.93 (m, 4H), 3.78 (t, J = 12.0 Hz, 2H), 3.63−3.55 (m, 2H), 3.53−3.46 (m, 4H), 1.49

(s, 6H), 1.18 (d, J = 6.2 Hz, 6H); HRMS: calcd for $C_{31}H_{36}FN_3O_5$ + H$^+$, 550.2712; found (ESI, [M + H]$^+$), 550.2712; Analytical HPLC: R_t = 10.4 min. (99.7%).

FXR, One Hybrid Assay. HEK293 stable clones expressing either Gal4/human FXR-LBD or Gal4/mouse FXR-LBD fusion protein in assay medium (Phenol red-free, high-glucose DMEM with 10% fetal bovine serum, 1 mM sodium pyruvate, 100 U/mL penicillin, 1% glutamax, and 100 g/mL streptomycin) were plated at 10 000 cells per well in 96-well plates in 50 μL assay medium. The cells were incubated at 37 °C for 2 h, and then 50 μL of the appropriate concentration of test compound in assay medium was added to each well. Cells treated with compounds were incubated for 24 h at 37 °C. On day 2, the medium was removed and lysis buffer added, and the plates were analyzed for luciferase activity with luciferase assay reagent (Promega E1483) and read on Victor3 V instrument (Perkin-Elmer) with the use of the luciferase assay protocol.

Mouse PK/PD Study. Eight-week-old male LDLR$^{-/-}$ mice were treated with 0.5% methylcellulose/2.0% Tween-80 (MC/T) vehicle (control) or 3 mg/kg **14cc** or **14dd**. Over a 24 h period, the mice were sacrificed (3 mice/time point/group) and plasma and liver samples were harvested. Total hepatic RNA was purified using the Qiagen RNeasy clean kit following the manufacturer's protocol, and gene expression of short heterodimer partner (SHP) was quantified by real-time RT-PCR with the Qiagen Quantitech kit using an ABI 7900. The relative amount of mRNA was normalized to 18S rRNA.

Mouse Dyslipidemia Model. Eight-week-old male LDLR$^{-/-}$ mice (six mice/group) were purchased from Jackson Laboratories and maintained on a chow diet. The mice were fed a Western diet (AIN-76A, Purina Test Diets) and treated by daily oral gavage with MC/T vehicle or varying concentrations of **14cc** or **14dd** as indicated for 7 days. On the last day after the final dose, the food was removed to allow a 3 h fast, and serum was harvested for analysis. Serum VLDLc, LDLc, and HDLc were determined by FPLC as previously described.[23]

Rhesus Monkey Model. Female monkeys (Covance Laboratories) (three monkeys/group) on a standard diet were treated by daily oral gavage with MC/T vehicle or 60 mg/kg of **14cc** for 28 days. Serum was harvested every 7 days and on the final day, livers were harvested for gene expression analysis. Serum TG and cholesterol levels were determined using a Roche 912 clinical chemistry analyzer and expressed as mg/dL. Serum VLDLc, LDLc, and HDLc and hepatic gene expression were determined as described above.

References

(1) (a) Forman, B. M.; Goode, E.; Chen, J.; Oro, A. E.; Bradley, D. J.; Perlmann, T.; Noonan, D. J.; Burka, L. T.; McMorris, T.; Lamph, W. W.; Evans, E. M.; Weinberger, C. Identification of a nuclear receptor that is activated by farnesol metabolites. *Cell* **1995**, *81*, 687–693. (b) Zhang, Y.; Kast-Woelbern, H. R.; Edwards, P. A. Natural structural variants of the nuclear receptor farnesoid X receptor affect transcriptional activation. *J. Biol. Chem.* **2003**, *278*, 101–110. (c) Otte, K.; Kranz, H.; Kober, I.; Thompson, P.; Hoefer, M.; Haubold, B.; Remmel, B.; Voss, H.; Kaiser, C.; Albers, M.; Cheruvallath, Z.; Jackson, D.; Casari, G.; Koegl, M.; Paabo, S.; Mous, J.; Kremoser, C.; Deuschle, U. Identification of farnesoid X receptor β as a novel mammalian nuclear receptor sensing lanosterol. *Mol. Cell. Biol.* **2003**, *23*, 864–872.

(2) (a) Makishima, M.; Okamoto, A. Y.; Repa, J. J.; Tu, H.; Learned, R. M.; Luk, A.; Hull, M. V.; Lustig, K. D.; Mangelsdorf, D. J.; Shan, B. Identification of a nuclear receptor for bile acids. *Science* **1999**, *284*, 1362–1365. (b) Parks, D. J.; Blanchard, S. G.; Bledsoe, R. K.; Chandra, G.; Consler, T. G.; Kliewer, S. A.; Stimmel, J. B.; Willson, T. M.; Zavacki, A. M.; Moore, D. D.; Lehmann, J. M. Bile acids: natural ligands for an orphan nuclear receptor. *Science* **1999**, *284*, 1365–1368.

(3) (a) Pellicciari, R.; Costantino, G.; Fiorucci, S. Farnesoid X receptor: From structure to potential clinical applications. *J. Med. Chem.* **2005**, *48*, 5383–5403. (b) Rizzo, G.; Renga, B.; Antonelli, E.; Passeri, D.; Pellicciari, R.; Fiorucci, S. The methyl transferase PRMT1 functions as co-activator of farnesoid X receptor (FXR)/9-cis retinoid X receptor and regulates transcription of FXR responsive genes. *Mol. Pharmacol.* **2005**, *68*, 551–555.

(4) Sinal, C. J.; Tohkin, M.; Miyata, M.; Ward, J. M.; Lambert, G.; Gonzalez, F. J. Targeted disruption of the nuclear receptor FXR/BAR impairs bile acid and lipid homeostasis. *Cell* **2000**, *102*, 731–744.

(5) Claudel, T.; Staels, B.t; Kuipers, F. The farnesoid X receptor: A molecular link between bile acid and lipid and glucose metabolism. *Arterioscler. Thromb. Vasc. Biol.* **2005**, *25*, 2020–2030.

(6) Hirokane, H.; Nakahara, M.; Tachibana, S.; Shimizu, M.; Sato, R. Bile acid reduces the secretion of VLDL by repressing microsomal triglyceride transfer protein gene expression mediated by hepatocyte nuclear factor-4. *J. Biol. Chem.* **2004**, *279*, 45685–45692.

(7) Bell, G. D.; Lewis, B.; Petrie, A.; Dowling, R. H. Serum lipids in cholelithiasis: Effect of chenodeoxycholic acid therapy. *Br. Med. J.* **1973**, *3*, 520–523.

(8) Angelin, B.; Hershon, K. S.; Brunzell, J. D. Bile acid metabolism in hereditary forms of hypertriglyceridemia: Evidence for an increased synthesis rate in monogenic familial hypertriglyceridemia. *Proc. Natl. Acad. Sci. U. S. A.* **1987**, *84*, 5434–5438.

(9) Angelin, B.; Einarsson, K.; Hellstrom, K.; Leijd, B. Effects of chenodeoxycholic acid on the metabolism of endogenous triglyceride and hyperlipoproteinemia. *J. Lipid Res.* **1978**, *19*, 1017–1024.

(10) Chawla, A.; Repa, J. J.; Evans, R. M.; Mangelsdorf, D. J. Nuclear receptors and lipid physiology: Opening the X-files. *Science* **2001**, *294*, 1866–1870.

(11) Yu, L.; Gupta, S.; Xu, F.; Liverman, A. D. B.; Moschetta, A.; Mangelsdorf, D. J.; Repa, J. J.; Hobbs, H. H.; Cohen, J. C. Expression of ABCG5 and ABCG8 is required for regulation of biliary cholesterol secretion. *J. Biol. Chem.* **2005**, *280*, 8742–8747.

(12) Evans, M. J.; Mahaney, P. E.; Borges-Marcucci, L.; Lai, K.-D.; Wang, S.; Krueger, J. A.; Gardell, S. J.; Huard, C.; Martinez, R.; Vlasuk, G. P.; Harnish, D. C. A synthetic farnesoid X receptor (FXR) agonist promotes cholesterol lowering in models of dyslipidemia. *Am. J. Physiol. Gastrointest. Liver Physiol.* **2009**, *296*, G543–G552.

(13) Maloney, P. R.; Parks, D. J.; Haffner, C. D.; Fivush, A. M.; Chandra, G.; Plunket, K. D.; Creech, K. L.; Moore, L. B.; Wilson, J. G.; Lewis, M. C.; Jones, S. A.; Willson, T. M. Identification of a chemical tool for the orphan nuclear receptor FXR. *J. Med. Chem.* **2000**, *43*, 2971–2974.

(14) Nicolaou, K. C.; Evans, R. M.; Roecker, A. J.; Hughes, R.; Downes, M.; Pfefferkorn, J. A. Discovery and optimization of non-steroidal FXR agonists from natural product-like libraries. *Org. Biomol. Chem.* **2003**, *1*, 908–920.

(15) Pellicciari, R.; Fiorucci, S.; Camaioni, E.; Clerici, C.; Costantino, G.; Maloney, P. R.; Morelli, A.; Parks, D. J.; Willson, T. M. 6-Alpha-ethyl-chenodeoxycholic acid (6-ECDCA), a potent and selective FXR agonist endowed with anticholestatic activity. *J. Med. Chem.* **2002**, *45*, 3569–3572.

(16) Flatt, B.; Martin, R.; Wang, T.-L.; Mahaney, P.; Murphy, B.; Gu, X.-H.; Foster, P.; Li, J.; Pircher, P.; Petrowski, M.; Schulman, I.; Westin, S.; Wrobel, J.; Yan, G.; Bischoff, E.; Daige, C.; Mohan, R. Discovery of XL335 (WAY-362450): A highly potent, selective, and orally active agonist of the Farnesoid X Receptor (FXR). *J. Med. Chem.* **2009**, *52*, 904–907.

(17) Mehlmann, J. F.; Crawley, M. L.; Lundquist, J. T., IV; Unwalla, R. J.; Harnish, D. C.; Evans, M. J.; Kim, C. Y.; Wrobel, J. E.; Mahaney, P. E. Pyrrole[2,3-d]azepino compounds as agonists of the farnesoid X receptor (FXR). *Bioorg. Med. Chem. Lett.* **2009**, *19*, 5289–5292.

(18) Di, L.; Kerns, E.; Li, S.; Petusky, S. High throughput metabolic stability assay for insoluble compounds. *Int. J. Pharm.* **2006**, *317*, 54–60.

(19) Bohl, C.; Miller, D. D.; Chen, J.; Bell, C.; Dalton, J. Structural basis for accomodation of nonsteroidal ligans in the androgen receptor. *J. Biol. Chem.* **2005**, *280*, 37747–37754.

(20) Faernegardh, M.; Bonn, T.; Sun, S.; Ljunggren, J.; Ahola, H.; Wilhelmsson, A.; Gustafsson, J.-A.; Carlquist, M. The three-dimensional structure of the liver X receptor β reveals a flexible ligand-binding pocket that can accommodate fundamentally different ligands. *J. Biol. Chem.* **2003**, *278*, 38821–38828.

(21) Langhi, C.; Le May, C.; Kourimate, S.; Caron, S.; Staels, B.; Krempf, M.; Costet, P.; Cariou, B. Activation of the farnesoid

X receptor represses PCSK9 expression in human hepatocytes. *FEBS Lett.* **2008**, *582*, 949–955.

(22) Sanyal, S.; Bavner, A.; Haroniti, A.; Nilsson, L.-M.; Lundasen, T.; Rehnmark, S.; Witt, M. R.; Einarsson, C.; Talianidis, I.; Gustafsson, J.-A.; Treuter, E. Involvement of corepressor complex subunit GPS2 in transcriptional pathways governing human bile

acid biosynthesis. *Proc. Natl. Acad. Sci. U. S. A.* **2007**, *104*, 15665–15670.

(23) Quinet, E. M.; Savio, D. A.; Halpern, A. R.; Chen, L.; Schuster, G. U.; Gustafsson, J. A.; Basso, M. D.; Nambi, P. Liver X receptor LXR-beta regulation in LXR-alpha-deficient mice: implications for therapeutic targeting. *Mol. Pharmacol.* **2006**, *70*, 1340–1349.